NACA TN 2806

NATIONAL ADVISORY COMMITTEE FOR AERONAUTICS

TECHNICAL NOTE 2806

COMPARISON OF TWO- AND THREE-DIMENSIONAL POTENTIAL-FLOW SOLUTIONS IN A ROTATING IMPELLER PASSAGE

By Gaylord O. Ellis and John D. Stanitz

Lewis Flight Propulsion Laboratory
Cleveland, Ohio

Washington
October 1952

NATIONAL ADVISORY COMMITTEE FOR AERONAUTICS

TECHNICAL NOTE 2806

COMPARISON OF TWO- AND THREE-DIMENSIONAL POTENTIAL-FLOW SOLUTIONS IN A ROTATING IMPELLER PASSAGE

By Gaylord O. Ellis and John D. Stanitz

SUMMARY

A solution is presented for three-dimensional, incompressible, nonviscous, potential flow in a rotating impeller passage with zero through flow. The solution is obtained for a conventional impeller with straight blades but with the inducer vanes removed and the impeller blades extended upstream parallel to the axis of the impeller. By superposition of solutions two additional examples are obtained for different ratios of compressor flow rate to impeller tip speed. The three-dimensional solutions are compared with corresponding two-dimensional solutions and it is concluded that, at least for the type of impeller geometry investigated, two-dimensional solutions can be combined to describe the three-dimensional flow in rotating impellers with sufficient accuracy for engineering analyses.

INTRODUCTION

As an aid to better understanding of flow conditions in rotating impeller passages, methods of analysis have been developed in the past for potential nonviscous flow. In order to achieve solutions with a reasonable expenditure of effort, all methods are based on two-dimensional assumptions, in that the flow is restricted, by assumption, to specified flow surfaces in space. Either of two types of surface are usually assumed for the flow: first, the mean blade (or passage) surface on which flow conditions vary from hub to shroud but are considered constant in the circumferential direction (axial-symmetry solutions, references 1 and 2), or, second, surfaces of revolution on which flow conditions vary from one blade to the next, but normal to which the flow conditions are considered constant (blade-to-blade solutions, references 3 and 4).

If the streamlines of an axial symmetry solution are used to generate surfaces of revolution around the axis of the impeller, the totality of the blade-to-blade solutions on these surfaces of revolution

constitute a quasi-three-dimensional solution (reference 5) because the solutions indicate variations in flow conditions throughout the impeller passage. However, because the flow is constrained to surfaces of revolution, the solution is not three dimensional in the exact sense of the word. No complete three-dimensional solutions for rotating impeller passages exist in the literature, and a solution has therefore been obtained at the NACA Lewis laboratory. The solution is presented in this report and is compared with the results of axial-symmetry and blade-to-blade solutions in order to evaluate these two-dimensional methods of analysis.

The three-dimensional solution was obtained for incompressible nonviscous flow in a rotating impeller passage with straight blades and with the inducer vanes located far upstream of the impeller. By superposition of solutions, results are obtained for several ratios of flow rate to impeller tip speed.

GENERAL METHOD OF ANALYSIS

A partial differential equation for three-dimensional flow in a rotating impeller passage is developed from considerations of continuity and absolute irrotational fluid motion.

Assumptions. - The fluid is assumed to be inviscid and incompressible. The flow is assumed to be steady relative to the rotating impeller passage, and in the absence of viscosity the absolute motion of the fluid is assumed to be irrotational. It is assumed that the phenomenon being investigated, that is, the deviation of three-dimensional flow from the restricted motion of two-dimensional solutions, is qualitatively the same for compressible and incompressible solutions. This deviation is a perturbation resulting primarily from rotation of the impeller; and in reference 6 it is shown that at least for two-dimensional solutions this type of perturbation is independent of compressibility, which affects only the average velocity.

Cylindrical coordinate system and velocity components. - The cylindrical coordinates R, θ, and Z relative to the impeller are shown in figure 1(a). (All symbols are defined in appendix A.) These coordinates are dimensionless, the linear coordinates R and Z having been divided by the impeller tip radius (so that R is equal to 1.0 at the impeller tip).

The absolute velocity Q has components Q_R, Q_θ, and Q_Z in the R, θ, and Z directions, respectively (fig. 1(a)). These velocities are dimensionless, having been divided by the impeller tip speed (so that, for example, the dimensionless blade speed at any radius R is

equal to R). If W is the velocity of the fluid relative to the impeller, expressed as a ratio of the impeller tip speed, then

$$W_\theta = Q_\theta - R \tag{1}$$

Potential function φ. - For absolute irrotational fluid motion

$$\nabla \times \bar{Q} = 0 \tag{2}$$

where the bar indicates a vector quantity. A potential function φ satisfies equation (2) identically if defined by

$$\bar{Q} = \nabla \varphi \tag{3}$$

from which

$$\frac{\partial \varphi}{\partial R} = Q_R \tag{3a}$$

$$\frac{1}{R} \frac{\partial \varphi}{\partial \theta} = Q_\theta \tag{3b}$$

and

$$\frac{\partial \varphi}{\partial Z} = Q_Z \tag{3c}$$

Differential equation of flow. - From continuity

$$\nabla \cdot \bar{Q} = 0$$

so that, from equation (3),

$$\nabla^2 \varphi = 0 \tag{4a}$$

which in cylindrical coordinates becomes

$$\frac{\partial^2 \varphi}{\partial R^2} + \frac{1}{R} \frac{\partial \varphi}{\partial R} + \frac{1}{R^2} \frac{\partial^2 \varphi}{\partial \theta^2} + \frac{\partial^2 \varphi}{\partial Z^2} = 0 \tag{4b}$$

NUMERICAL PROCEDURE

A numerical procedure is outlined for the solution of the partial differential equation (4) for flow in a rotating impeller passage with special type of geometry.

Preliminary Considerations

Special type of impeller geometry. - The three-dimensional solutions presented are for a straight-bladed impeller of conventional design except that the inducer vanes are removed and the straight impeller blades are extended indefinitely upstream parallel to the axis of the compressor. This idealized entrance condition along with straight blades results in substantial simplification of the numerical procedure.

Superposition of solutions. - As a result of the special type of impeller geometry just discussed, the boundary conditions for flow through a rotating impeller are equal to the sum of the boundary conditions for zero flow through the rotating impeller and for finite flow through the stationary impeller. Therefore, because the boundary conditions can be added and because the differential equation (4) is linear, the velocity potential φ for flow through the rotating impeller passage can be expressed as

$$\varphi = \varphi_1 + k\varphi_2 \tag{5}$$

where φ_1 satisfies equation (4) and the boundary conditions for the rotating impeller with zero net through flow and φ_2 satisfies the same equation but for the boundary conditions associated with flow through the stationary impeller. The solution for φ_1 is called the "eddy-flow solution" and corresponds to ideal flow conditions in the rotating impeller with the throttle closed so that no through flow occurs. The solution for φ_2 is called the "through-flow solution" and, for the special type of impeller geometry being considered, this solution is axially symmetric and corresponds to flow with zero whirl through an annulus with the same hub-shroud profile and no impeller blades. Solutions for various ratios of flow rate to impeller tip speed are obtained directly for various values of k in equation (5).

Eddy-Flow Solution

The eddy-flow solution for the rotating impeller passage with zero net through flow is considered first.

Transformation of coordinates. - It is convenient for purposes of the numerical solution by relaxation methods to transform the RZ-plane to one on which the coordinates are the streamlines η and velocity potential lines ξ for flow through the compressor annulus without blades. Because the hub and shroud contours are streamlines in the RZ-plane, these contours become straight parallel lines in the $\xi\eta$-plane. In terms of the new transformed coordinates, equation (4b) for the eddy-flow potential φ_1 becomes (appendix B)

$$Q_2^2 \frac{\partial^2 \varphi_1}{\partial \xi^2} + R^2 Q_2^2 \frac{\partial^2 \varphi_1}{\partial \eta^2} + \frac{1}{R^2} \frac{\partial^2 \varphi_1}{\partial \theta^2} + 2(Q_2)_Z \frac{\partial \varphi_1}{\partial \eta} = 0 \tag{6}$$

where the subscript 2 refers to the solution for axially symmetric flow through the compressor annulus with no blades or, which is the same thing, through the stationary impeller passage of the special type considered in this report.

The new coordinate system introduces two additional velocity components (appendix B)

$$Q_\xi = Q_2 \frac{\partial \varphi}{\partial \xi} \tag{7a}$$

and

$$Q_\eta = R Q_2 \frac{\partial \varphi}{\partial \eta} \tag{7b}$$

and an angle α_2 defined by

$$\tan \alpha_2 = \left(\frac{Q_R}{Q_Z} \right)_2 \tag{8}$$

all of which are shown in figure 1(b). From this figure it is seen that

$$Q_\xi = Q_Z \cos \alpha_2 + Q_R \sin \alpha_2 \tag{9a}$$

and

$$Q_\eta = Q_R \cos \alpha_2 - Q_Z \sin \alpha_2 \tag{9b}$$

or, conversely,

$$Q_R = Q_\xi \sin \alpha_2 + Q_\eta \cos \alpha_2 \tag{10a}$$

and

$$Q_Z = Q_\xi \cos \alpha_2 - Q_\eta \sin \alpha_2 \tag{10b}$$

Boundary conditions. - For the eddy-flow solution of equation (6) the boundary conditions that must be satisfied for the special type of impeller geometry considered in this report are:

(1) The flow direction must be tangent to the hub and shroud in the impeller and diffuser so that Q_η is zero, or, from equation (7b),

$$\frac{\partial \varphi}{\partial \eta} = 0 \tag{11}$$

(2) Along the blade the relative flow is tangent to the blade surface so that for straight radial blades the relative tangential velocity W_θ is zero and from equations (1) and (3b)

$$\frac{\partial \varphi}{\partial \theta} = R^2$$

(3) Boundaries are established in the diffuser on meridional planes extending from the blade tips. For a rotating impeller with no through flow the radial velocity component is zero on these boundaries so that the potential function is constant along radial lines on these surfaces. Variations in velocity potential φ with Z at the impeller tip of constant radius indicate the presence of a vortex sheet shedding from the trailing edge of the blade and passing downstream. It is assumed that the strength of this sheet is weak and can be ignored in the solution of equation (6). For impeller blades with constant tip radius the variation in work input from hub to shroud at the impeller tip is negligible and the assumption therefore appears to be reasonable. The Joukowski condition at the blade tip is automatically satisfied by condition (2).

(4) The domain of the solutions is extended in the upstream and downstream directions until flow conditions are uniform in a plane normal to the direction of through flow. For the eddy-flow solution this condition is achieved when $(Q_1)_\xi$ is zero, that is, when $\partial \varphi_1 / \partial \xi$ is zero, everywhere on a plane normal to the ξ coordinate.

(5) The idealized inlet of the special impeller geometry considered in this report results in symmetry of flow about the mean plane between blades in the rotating impeller with no through flow. The flow is directed normal to this plane and φ_1 is therefore everywhere constant (zero) on it.

Relaxation solution. - The differential equation (6) is solved by relaxation methods (reference 7) to satisfy the boundary conditions just described. The velocity components are then determined by equations (3) and (7) in finite difference form. For the numerical examples of this report, a three-point system was used for expressing the differential equations in finite difference form.

Flow paths. - Any three velocity components determine the flow direction at a point so that flow paths relative to the impeller passage can be determined from the velocity components Q_R, W_θ, and Q_Z, or Q_ξ, W_θ, and Q_η. On the hub, shroud, and blade surfaces the path lines can be constructed graphically from lines of constant flow direction on these surfaces.

Accuracy. - For the numerical examples of this report, the impeller channel includes a total of 5400 grid points at which the velocity potential was relaxed to a unit change in the fifth decimal. (Because φ_1 is constant on the mean plane and the flow is symmetrical about this plane, the number of grid points at which it was necessary to relax is reduced to 2400.)

In order to check the accuracy of the graphical construction of the path lines, these lines were obtained on a plane normal to the through-flow direction far upstream of the impeller where a direct two-dimensional solution for the stream function is known and valid. Figure 2(a) compares the path lines with the streamlines. It is noted that the graphically constructed path lines agree well with the streamlines. It should be pointed out, however, that the path-line spacing is not sufficiently accurate to be indicative of the velocity distribution. In figure 2(b) the velocities obtained from the three-dimensional solution for the velocity potential are compared with the velocities obtained from the two-dimensional solution for the stream function. The comparison indicates much better agreement in the velocity distributions than was indicated by the path-line spacing in figure 2(a).

A check on the accuracy of the three-dimensional solution will be given in connection with a discussion of the numerical examples. This check indicates approximately the same accuracy that is shown by the comparison of velocities in figure 2(b).

Combined Solutions

After the eddy-flow solution has been obtained, various percentages of a through-flow solution may be added to obtain solutions for different ratios of compressor flow rate to impeller tip speed.

Through-flow solution. - The through-flow solution is obtained by methods outlined in reference 1, for example. As already discussed, the velocity potentials for the two types of solution can be added or, as indicated by partial derivatives of φ in equation (5), the velocity components themselves can be added directly. The latter procedure avoids the necessity of computing the distribution of φ_2 from the distribution of stream function determined by reference 1.

Flow path. - The procedure for graphically determining the flow path for the combined solutions is identical with that outlined for the eddy-flow solution.

NUMERICAL EXAMPLES

Three-dimensional solutions for flow through an impeller with straight blades and with the inducer vanes located far upstream of the impeller are presented for: (1) zero flow through the rotating impeller passage, (2) flow through the stationary impeller passage, and (3) combinations of (1) and (2) for various ratios of through flow to impeller tip speed.

Impeller Geometry

The impeller geometry for the numerical examples is the same as that in references 1 and 4 with the inducer vanes located far upstream of the impeller. The hub-shroud profile of the impeller is described in figure 3. The blade spacing is 32.80° as in reference 4.

The results of the solutions are presented on the channel surfaces and on the nine meridional planes indicated in figure 4(a). The ξ,η coordinates on the meridional planes are shown in figure 4(b). The lines of constant ξ are spaced at intervals corresponding to equal increments of the ξ coordinate used in reference 4.

Solution for Zero Net Flow Through Rotating Impeller Passage

Velocity potential φ_1. - Lines of constant velocity potential on the meridional planes are shown in figure 5. The center plane E (see fig. 4(a)) is not shown because, as discussed previously, φ_1 is zero everywhere on this plane. Note that lines of constant φ_1 intersect the hub-shroud profile at right angles, as required by equation (11). The meridional velocity component must be directed normal to the lines of constant φ_1 in the meridional planes and has magnitudes inversely proportional to the line spacings.

Velocity components. - Velocity components of the eddy-flow solution are shown in figures 6 to 8. These velocity components are directly related by equation (3) to the local partial derivatives of the velocity potential φ_1 given in figure 5. For the impeller geometry being investigated, all these eddy-flow velocity components would be neglected by axial-symmetry-type solutions (reference 1).

Lines of constant $(Q_1)_\xi$ on the meridional planes are shown in figure 6. This velocity component of the eddy-flow solution is tangent to the streamlines (constant η), and therefore to the velocities, of the axially symmetric flow through the stationary impeller. The velocity component $(Q_1)_\xi$ has maximum values on the blade surfaces (planes A and A') and is zero on the center plane E. This velocity component also becomes zero upstream and downstream of the impeller proper.

Lines of constant velocity component $(Q_1)_\eta$ are shown on the meridional planes in figure 7. This velocity component of the eddy-flow solution is normal to the streamlines, and therefore to the velocities, of the flow through the stationary impeller. The velocity component $(Q_1)_\eta$ has maximum values on the blade surfaces and is zero on the center plane E. This velocity component must also be zero along the hub and shroud boundaries, and becomes zero downstream of the impeller. Note that the velocity component $(Q_1)_\eta$ would be completely neglected in two-dimensional solutions on surfaces of revolution (reference 4) generated by streamlines of axial-symmetry-type solutions.

Lines of constant tangential velocity component $(W_1)_\theta$ relative to the impeller are shown in figure 8. For the impeller geometry investigated, this velocity component has maximum values on the center plane E and is zero on the blade surfaces. Negative values of $(W_1)_\theta$ indicate flow across the meridional planes in the direction opposed to impeller rotation (into the page), and positive values of $(W_1)_\theta$ indicate flow across the meridional planes in the direction of rotation (out of the page). From continuity considerations the integrated weight flow into the page (exclusive of the fluid that remains in the diffuser) must equal the integrated weight flow out of the page. These integrations have been carried out for the center plane E and weight flows agree within $2\frac{1}{2}$ percent. This agreement indicates approximately the same accuracy as that obtained from the integrated weight flows across the center line in figure 2(b). Thus it seems reasonable to conclude that the error throughout the domain of the three-dimensional solution is not greater than that indicated by the velocities in figure 2(b).

Path lines. - Path lines of fluid particles on the passage surfaces are shown for the eddy-flow solution in figure 9. The fluid remains in the impeller passage and rotates in the opposite direction to that of the impeller.

Solution for Flow Through Stationary Impeller Passage

Flow through a stationary impeller with straight blades has zero tangential velocity and is equivalent to flow through the annulus formed by the hub and shroud surfaces. In reference 1, it is shown that for

incompressible flow the distributions of stream function and velocity components in the meridional plane for flow through an annulus are the same as the distributions for axially symmetric flow through a rotating impeller with an infinite number of straight impeller blades. Therefore, example II of reference 1 is used in this report as the solution for flow through the stationary impeller passage.

Streamlines. - Streamlines for flow through the stationary impeller passage are shown in figure 10. These lines are also the η coordinates (fig. 4(b)) used in the relaxation solution for the eddy flow.

Velocity distribution. - For flow through the stationary impeller passage, $(Q_2)_\theta$, $(W_2)_\theta$, and $(Q_2)_\eta$ are zero. Lines of constant velocity $(Q_2)_\xi$ (equal to Q_2) are shown on a meridional plane in figure 11. As for the eddy-flow solution, this velocity is expressed as a ratio of the tip speed of the rotating impeller, and the solution presented was obtained for $(Q_2)_\xi$ equal to 0.3429 far upstream of the impeller proper. The distribution of $(Q_2)_\xi$ is the same for all meridional planes.

Flow direction. - Lines of constant flow direction α_2 are shown on a meridional plane in figure 12. These values of α_2 can be used to compute the velocity components Q_R and Q_Z by equation (10).

Solutions for Flow Through Rotating Impeller Passage

Solutions for various ratios of flow rate to impeller tip speed are obtained by superposition of various percentages (k in equation (5)) of the through-flow solution on the eddy-flow solution. Either the velocity potential or the velocity components may be superposed. Two solutions are presented for flow through the rotating impeller with values of the axial inlet velocity Q_Z (equal to $(Q_2)_\xi$) upstream of the impeller equal to 0.1372 and 0.3429, that is, for k equal to 0.4 and 1.0, respectively.

Solution for k = 0.4. - Path lines of fluid particles on the surfaces of the impeller channel are shown in figure 13 for 40 percent of the through-flow solution superposed on the eddy-flow solution. Path lines on the hub and on the blade surface faced in the direction of rotation are shown in figure 13(a); path lines on the shroud and on the blade surface opposed to the direction of rotation are shown in figure 13(b). A composite plot of these path lines is shown in figure 13(c).

For this solution the flow rate through the rotating impeller is not sufficient to eliminate (by superposition) all the reverse flow resulting from the negative velocities $(Q_1)_\xi$ of the eddy-flow solution (see fig. 7(a)). This condition corresponds to the eddy flow that is attached

to the face of the blade in the direction of rotation for two-dimensional solutions on surfaces of revolution (references 4 and 6, for example). Unlike the two-dimensional solutions, however, the fluid in the reverse flow of the three-dimensional solution does not remain in the impeller but eventually leaves as indicated by the spiral path lines emanating from the stagnation point on the hub of the impeller.

The locus of stagnation points indicated on the blade surface in figure 13(a) corresponds to the downstream stagnation point associated with the eddy flow of a two-dimensional solution. For the three-dimensional solution in figure 13(a), upstream stagnation points occur at the hub and shroud only. However, along the dot-dash line between these stagnation points the velocity component Q_ξ is zero so that this line corresponds to the upstream stagnation point associated with the eddy flow of a two-dimensional solution. Path lines on the shroud surface in figure 13(b) converge to the upstream stagnation point. This convergence indicates that, as the path lines approach the stagnation point, the fluid leaves the shroud surface and passes into the interior of the passage.

Solution for $k = 1.0$. - Path lines of fluid particles on the surfaces of the impeller channel are shown in figure 14 for 100 percent of the through-flow solution superposed on the eddy-flow solution. The conditions for this solution are the same as those for the two-dimensional solutions given in references 1 and 4. Path lines on the hub and on the blade surface faced in the direction of rotation are shown in figure 14(a); path lines on the shroud and on the blade surface opposed to the direction of rotation are shown in figure 14(b). A composite plot of these path lines is shown in figure 14(c).

COMPARISON OF TWO- AND THREE-DIMENSIONAL SOLUTIONS

The results of the three-dimensional solution are compared with two-dimensional solutions on the mean passage surface extending from hub to shroud, on the mean surface of revolution, and on the shroud surface. Only the eddy-flow solutions are compared because the contribution of through flow to the velocity components is the same for both the two- and three-dimensional solutions. Thus the velocity components to be compared are components of the perturbation velocity caused by the rotation of the impeller, and the relative importance of errors in these components is reduced when the known, primary through flow is added.

Mean passage surface. - Because, for the type of impeller geometry investigated, the three-dimensional eddy flow has no velocity components in the mean passage surface extending from hub to shroud (plane E, fig. 4(a)), the velocity components in this plane are solely determined

by, and therefore agree with, the axial-symmetry two-dimensional solution. The axial-symmetry solution, however, completely neglects the relative tangential velocity W_θ, which for the three-dimensional solution has maximum values on the mean plane (fig. 8(d)).

For impellers with curved blades, the relative tangential velocity component reaches maximum values on a mean flow surface between the blades. If, as for high-solidity blade rows, this surface is not much different from the geometric mean surface between blades, then the flow is nearly two dimensional on the mean passage surface and the flow on this mean surface is approximately described by axial-symmetry solutions like those of reference 1. This conclusion is reached by Ruden in reference 8.

Mean surface of revolution. - The velocity components Q_ξ and W_θ for the two- and three-dimensional solutions are compared on the mean surface of revolution in figures 15 and 16. The agreement for Q_ξ in figures 15(a) and 15(b) is excellent, and the agreement for W_θ in figures 16(a) and 16(b) is also excellent near the impeller tip, although the two-dimensional solution (fig. 16(b)) introduces relatively small positive values of W_θ not found for the three-dimensional solution in the region upstream of the contour line for W_θ equal to zero.

The slip factor, defined as the ratio of average absolute tangential velocity at the impeller tip to the tip speed of the impeller, depends on the distribution of W_θ at the impeller tip and is equal to 0.7892 for the three-dimensional solution compared with 0.8142 for the two-dimensional solution on the mean surface of revolution (reference 4).

The velocity component Q_η of the three-dimensional solution is plotted in figure 17. This velocity component is normal to the mean surface of revolution and is completely neglected by the two-dimensional solution.

Shroud. - The velocity components Q_ξ and W_θ for the two- and three-dimensional solutions are compared on the shroud surface in figures 18 and 19. (The two-dimensional solution on the shroud surface was obtained from correlation equations, developed in reference 4, using, for "standard values" of velocity, the velocities of the two-dimensional, eddy-flow solution on the mean plane.) The agreement for Q_ξ in figures 18(a) and 18(b) is good, but the agreement for W_θ in figures 19(a) and 19(b) is poor, except in a limited region near the impeller tip. From simple physical considerations the agreement for Q_ξ and W_θ on the hub is expected to be similar to the agreement on the shroud, except that W_θ will have large positive values instead of the large negative values on the shroud. On the hub and shroud surfaces the velocity component Q_η is zero for both the two- and three-dimensional solutions.

Summary of comparisons. - A summary of the comparisons between the two- and three-dimensional solutions that are discussed in this report is given in the following table:

Velocity component	Agreement		
	Mean passage surface	Mean surface of revolution	Hub or shroud surface
Q_ξ	good	good	good
W_θ	poor	good	poor
Q_η	good	poor	good

It is concluded that on the flow surfaces investigated the velocity components Q_ξ, W_θ, and Q_η agree for the two- and three-dimensional solutions discussed in this report, except: (1) W_θ on the hub, shroud, and mean passage surface, and (2) Q_η on the mean surface of revolution.

If quasi-three-dimensional solutions are obtained by the proper combination of two-dimensional axial-symmetry and blade-to-blade solutions (reference 5), good agreement with the exact three-dimensional solution is indicated by good agreement on all surfaces of revolution. This agreement has already been discussed for the hub, shroud, and mean surfaces of revolution. For intermediate surfaces the table of comparisons suggests that the agreement will always be good for Q_ξ, will be progressively better for W_θ as the mean surface of revolution is approached, and will be progressively better for Q_η as the hub and shroud are approached. Because Q_ξ is the velocity component of prime importance, it is concluded that, at least for the type of impeller investigated in this report, two-dimensional solutions can be combined to describe the three-dimensional flow in rotating impeller passages with sufficient accuracy for engineering analyses.

SUMMARY OF RESULTS AND CONCLUSIONS

A solution is presented for three-dimensional, incompressible, nonviscous, potential flow in a rotating impeller passage with zero through flow. The solution is obtained for a conventional impeller with straight blades but with the inducer vanes removed and the impeller blades extended upstream parallel to the axis of the impeller. By superposition of solutions two additional examples are obtained for different flow

rates through the rotating impeller. Of particular interest is the fact that at low compressor flow rates the fluid in the reverse or eddy-flow region does not remain permanently in the impeller passage, as is the case for two-dimensional solutions on surfaces of revolution, but, after spiraling around, eventually leaves the impeller. In other respects the three-dimensional solutions are compared with corresponding two-dimensional solutions and it is concluded that, at least for the type of impeller geometry investigated, two-dimensional solutions can be combined to describe the three-dimensional flow in rotating impellers with sufficient accuracy for engineering analyses. In particular it is concluded that:

1. On the mean surface of revolution the velocity components, except the component normal to the surface, agree for the two- and three-dimensional solutions.

2. On the hub and shroud surfaces the relative tangential velocity component does not agree for two- and three-dimensional solutions, but the other velocity components do.

Lewis Flight Propulsion Laboratory
National Advisory Committee for Aeronautics
Cleveland, Ohio, July 3, 1952

APPENDIX A

SYMBOLS

The following symbols are used in this report:

$A,A',B,B',\ldots$	meridional planes (fig. 4(a))
k	percentage of through-flow solution φ_2
Q	absolute velocity, expressed as ratio of impeller tip speed
R,θ,Z	cylindrical coordinates (fig. 1(a)), linear coordinates expressed as ratios of impeller tip radius
W	relative velocity, expressed as ratio of impeller tip speed
α_2	angle, figure 1(b) and equation (8)
ξ,η	velocity potential and stream function, respectively, for incompressible flow through hub-shroud annulus; used as coordinate system in $\xi\eta$-plane, equations (B1) and (B2)
φ	velocity potential, equation (3)

Subscripts:

1	rotating impeller with zero net through flow (eddy-flow solution)
2	stationary impeller with through flow (for numerical example, through flow is such that Q_Z equals 0.3429 upstream of impeller)
R,θ,Z,ξ,η	components in R,θ,Z,ξ,η directions, respectively

APPENDIX B

TRANSFORMATION FROM RZ- TO $\xi\eta$-PLANE

It is convenient for purposes of solution by relaxation methods to transform the RZ-plane to one on which the coordinates are the stream function η and the velocity potential ξ for flow through the compressor annulus without blades. The stream function η satisfies the continuity condition if defined as

$$\left.\begin{aligned} \frac{\partial \eta}{\partial R} &= R(Q_2)_Z \\ \frac{\partial \eta}{\partial Z} &= -R(Q_2)_R \end{aligned}\right\} \tag{B1}$$

and the velocity potential ξ satisfies the irrotationality condition if defined as

$$\left.\begin{aligned} \frac{\partial \xi}{\partial R} &= (Q_2)_R \\ \frac{\partial \xi}{\partial Z} &= (Q_2)_Z \end{aligned}\right\} \tag{B2}$$

In terms of the transformed ξ,η coordinates, the partial derivatives of equation (4b) become

$$\left.\begin{aligned} \frac{\partial \varphi}{\partial R} &= \frac{\partial \varphi}{\partial \xi}\frac{\partial \xi}{\partial R} + \frac{\partial \varphi}{\partial \eta}\frac{\partial \eta}{\partial R} \\ \frac{\partial^2 \varphi}{\partial R^2} &= \frac{\partial^2 \varphi}{\partial \xi^2}\left(\frac{\partial \xi}{\partial R}\right)^2 + 2\frac{\partial^2 \varphi}{\partial \xi \partial \eta}\frac{\partial \xi}{\partial R}\frac{\partial \eta}{\partial R} + \frac{\partial^2 \varphi}{\partial \eta^2}\left(\frac{\partial \eta}{\partial R}\right)^2 + \\ &\quad \frac{\partial \varphi}{\partial \xi}\frac{\partial^2 \xi}{\partial R^2} + \frac{\partial \varphi}{\partial \eta}\frac{\partial^2 \eta}{\partial R^2} \\ \frac{\partial \varphi}{\partial Z} &= \frac{\partial \varphi}{\partial \xi}\frac{\partial \xi}{\partial Z} + \frac{\partial \varphi}{\partial \eta}\frac{\partial \eta}{\partial Z} \\ \frac{\partial^2 \varphi}{\partial Z^2} &= \frac{\partial^2 \varphi}{\partial \xi^2}\left(\frac{\partial \xi}{\partial Z}\right)^2 + 2\frac{\partial^2 \varphi}{\partial \xi \partial \eta}\frac{\partial \xi}{\partial Z}\frac{\partial \eta}{\partial Z} + \frac{\partial^2 \varphi}{\partial \eta^2}\left(\frac{\partial \eta}{\partial Z}\right)^2 + \\ &\quad \frac{\partial \varphi}{\partial \xi}\frac{\partial^2 \xi}{\partial Z^2} + \frac{\partial \varphi}{\partial \eta}\frac{\partial^2 \eta}{\partial Z^2} \end{aligned}\right\} \tag{B3}$$

From equations (B1) through (B3), equation (4b) becomes

$$(Q_R^2 + Q_Z^2)_2 \left(\frac{\partial^2 \varphi}{\partial \xi^2} + R^2 \frac{\partial^2 \varphi}{\partial \eta^2} \right) + \frac{1}{R^2} \frac{\partial^2 \varphi}{\partial \theta^2} + \left(\frac{\partial Q_R}{\partial R} + \frac{Q_R}{R} + \frac{\partial Q_Z}{\partial Z} \right)_2 \frac{\partial \varphi}{\partial \xi} +$$

$$\left[2(Q_2)_Z + R \left(\frac{\partial Q_Z}{\partial R} - \frac{\partial Q_R}{\partial Z} \right)_2 \right] \frac{\partial \varphi}{\partial \eta} = 0 \qquad \text{(B4)}$$

But,

$$(Q_R^2 + Q_Z^2)_2 = Q_2^2$$

and from continuity

$$\left(\frac{\partial Q_R}{\partial R} + \frac{Q_R}{R} + \frac{\partial Q_Z}{\partial Z} \right)_2 = 0$$

and for irrotational flow

$$\left(\frac{\partial Q_Z}{\partial R} - \frac{\partial Q_R}{\partial Z} \right)_2 = 0$$

so that equation (B4) becomes

$$Q_2^2 \frac{\partial^2 \varphi}{\partial \xi^2} + R^2 Q_2^2 \frac{\partial^2 \varphi}{\partial \eta^2} + \frac{1}{R^2} \frac{\partial^2 \varphi}{\partial \theta^2} + 2(Q_2)_Z \frac{\partial \varphi}{\partial \eta} = 0 \qquad (6)$$

Equation (6) is the partial differential equation for the distribution of φ in the ξ, η, θ coordinate system.

This new coordinate system introduces two new velocity components Q_ξ and Q_η, which are related to the radial and axial velocity components by equation (9). Combining equations (3), (9), and (B1) to (B3) gives

$$Q_\xi = Q_2 \frac{\partial \varphi}{\partial \xi} \qquad (7a)$$

$$Q_\eta = R Q_2 \frac{\partial \varphi}{\partial \eta} \qquad (7b)$$

REFERENCES

1. Ellis, Gaylord O., Stanitz, John D., and Sheldrake, Leonard J.: Two Axial-Symmetry Solutions for Incompressible Flow Through a Centrifugal Compressor With and Without Inducer Vanes. NACA TN 2464, 1951.

2. Hamrick, Joseph T., Ginsburg, Ambrose, and Osborn, Walter M.: Method of Analysis for Compressible Flow Through Mixed-Flow Centrifugal Impellers of Arbitrary Design. NACA TN 2165, 1950.

3. Stanitz, John D.: Two-Dimensional Compressible Flow in Turbomachines with Conic Flow Surfaces. NACA Rep. 935, 1949. (Supersedes NACA TN 1744.)

4. Stanitz, John D., and Ellis, Gaylord O.: Two-Dimensional Flow on General Surfaces of Revolution in Turbomachines. NACA TN 2654, 1952.

5. Stanitz, John D.: Approximate Design Method for High-Solidity Blade Elements in Compressors and Turbines. NACA TN 2408, 1951.

6. Stanitz, John D., and Ellis, Gaylord O.: Two-Dimensional Compressible Flow in Centrifugal Compressors with Straight Blades. NACA Rep. 954, 1950. (Supersedes NACA TN 1932.)

7. Southwell, R. V.: Relaxation Methods in Theoretical Physics. Clarendon Press, (Oxford), 1946.

8. Ruden, P.: Investigation of Single-Stage Axial Fans. NACA TM 1062, 1944.

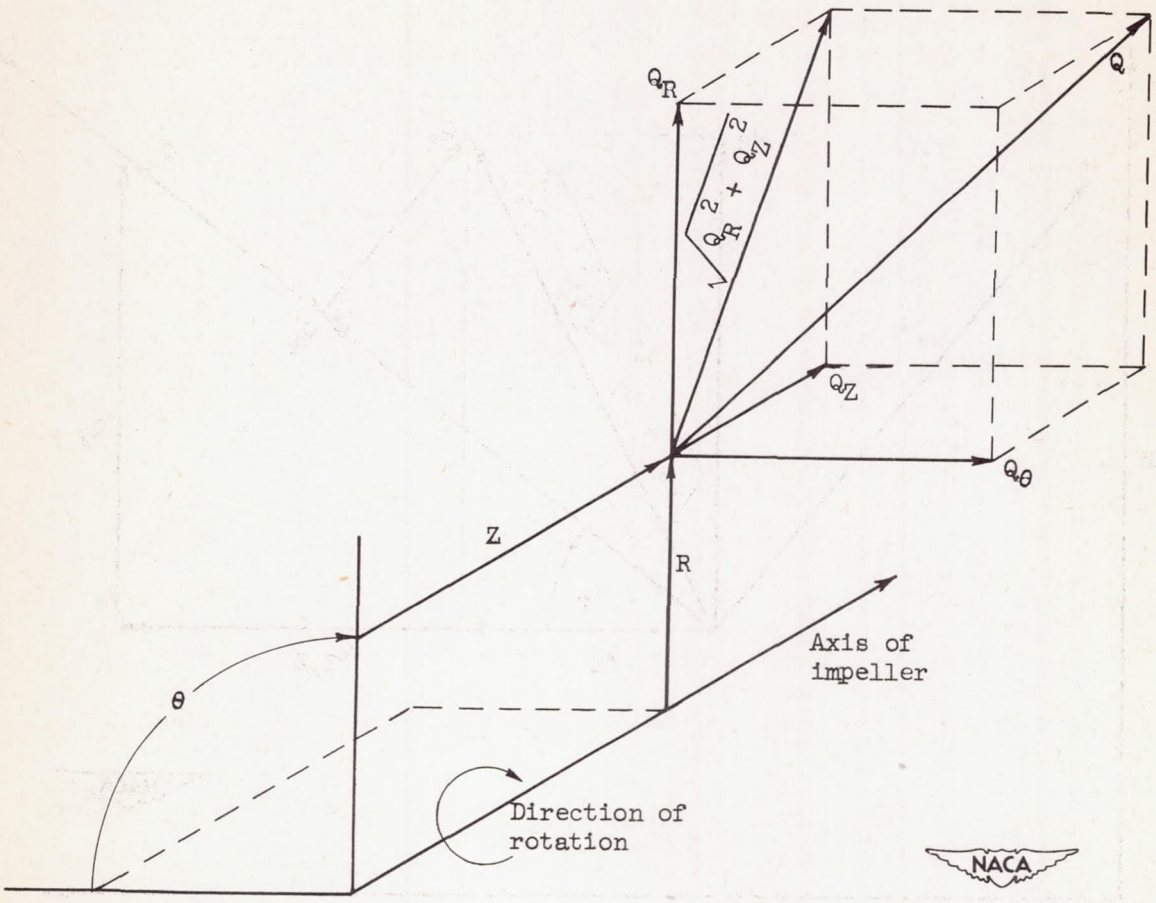

(a) Cylindrical coordinates.

Figure 1. - Coordinate systems relative to impeller, and absolute velocity components. All quantities are dimensionless. Linear coordinates are measured in units of impeller tip radius; velocity components are measured in units of impeller tip speed.

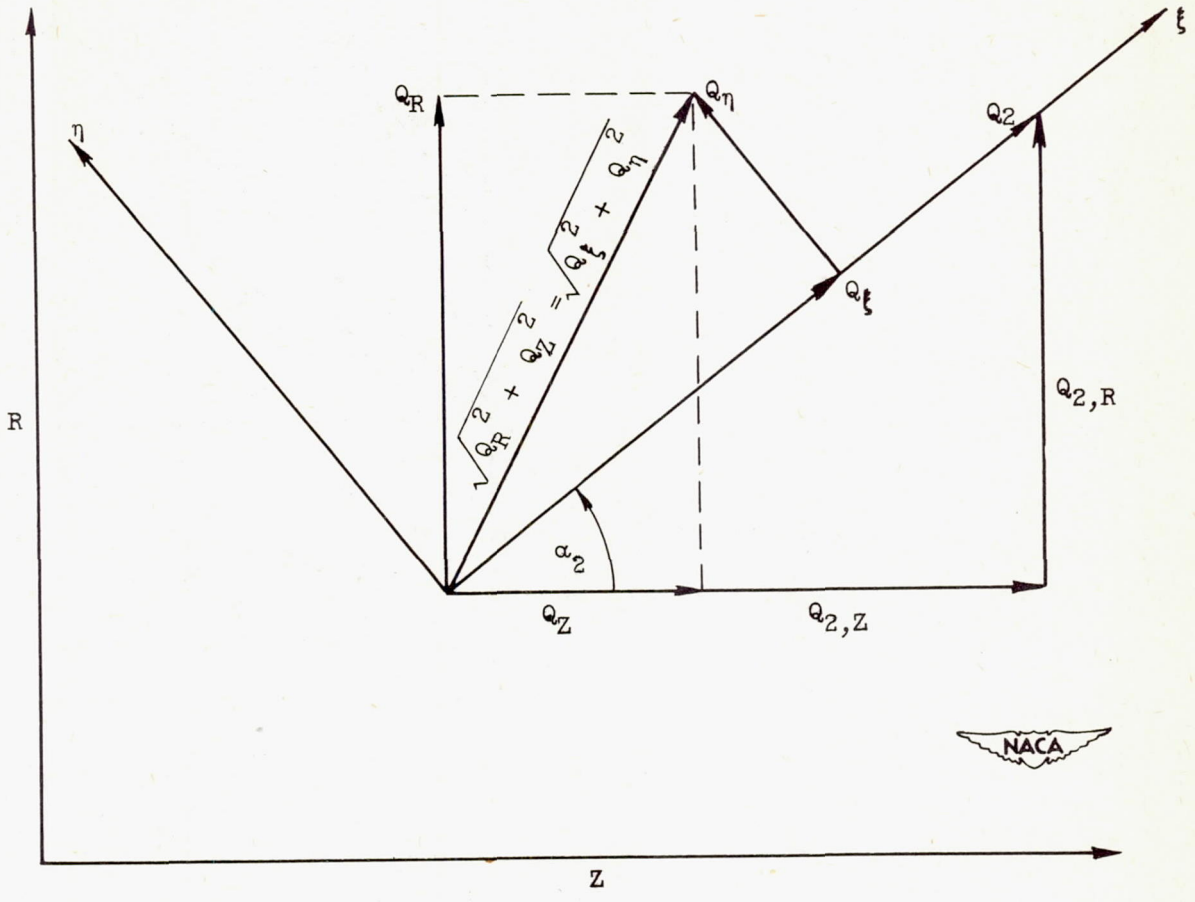

(b) ξ,η coordinate system in RZ-plane.

Figure 1. - Concluded. Coordinate systems relative to impeller, and absolute velocity components. All quantities are dimensionless. Linear coordinates are measured in units of impeller tip radius; velocity components are measured in units of impeller tip speed.

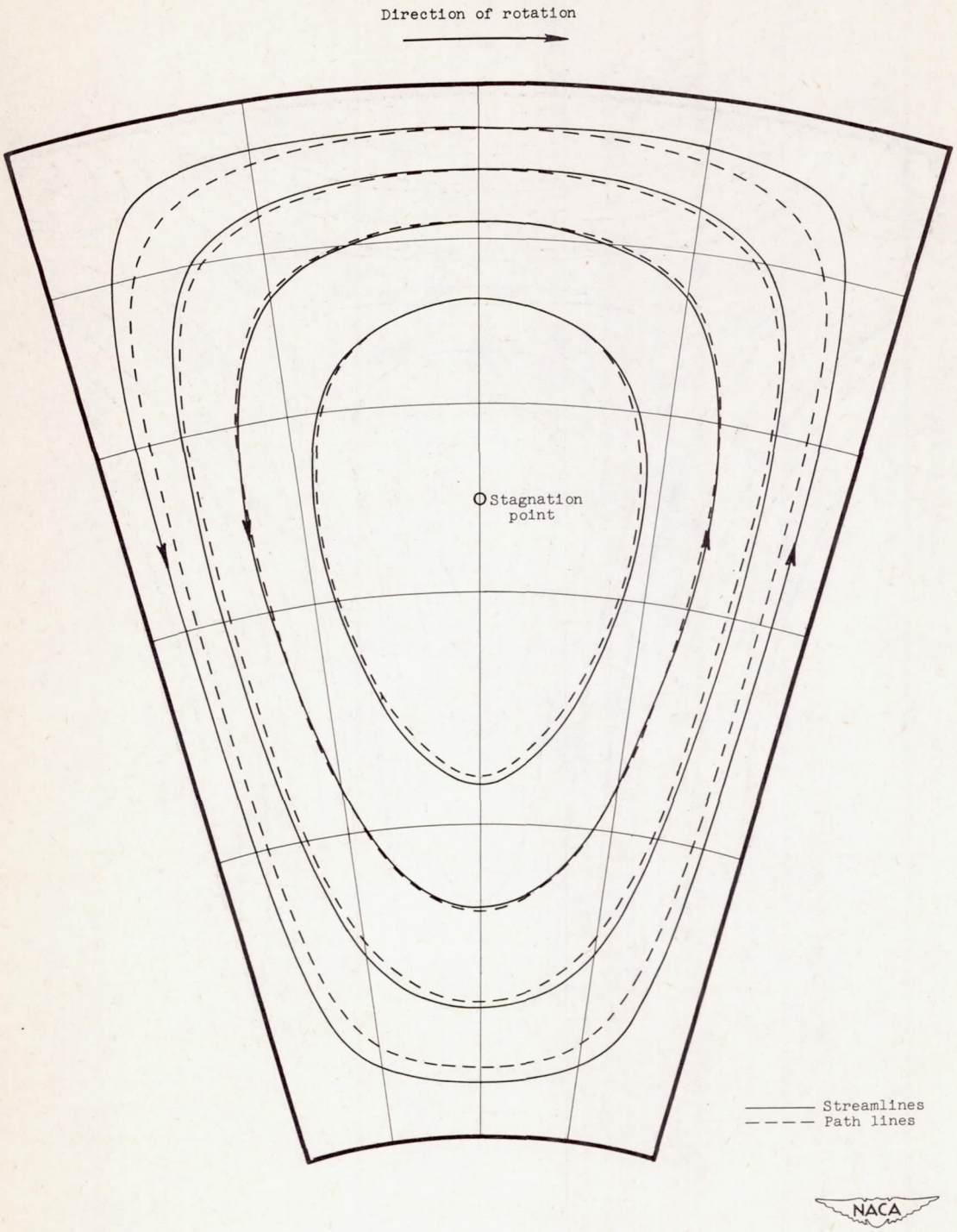

(a) Comparison of graphically constructed path lines (three-dimensional solution) with streamlines obtained from stream function of two-dimensional solution.

Figure 2. - Comparison of results obtained from two- and three-dimensional solutions. Plane normal to impeller axis in region of uniform axial velocity far upstream.

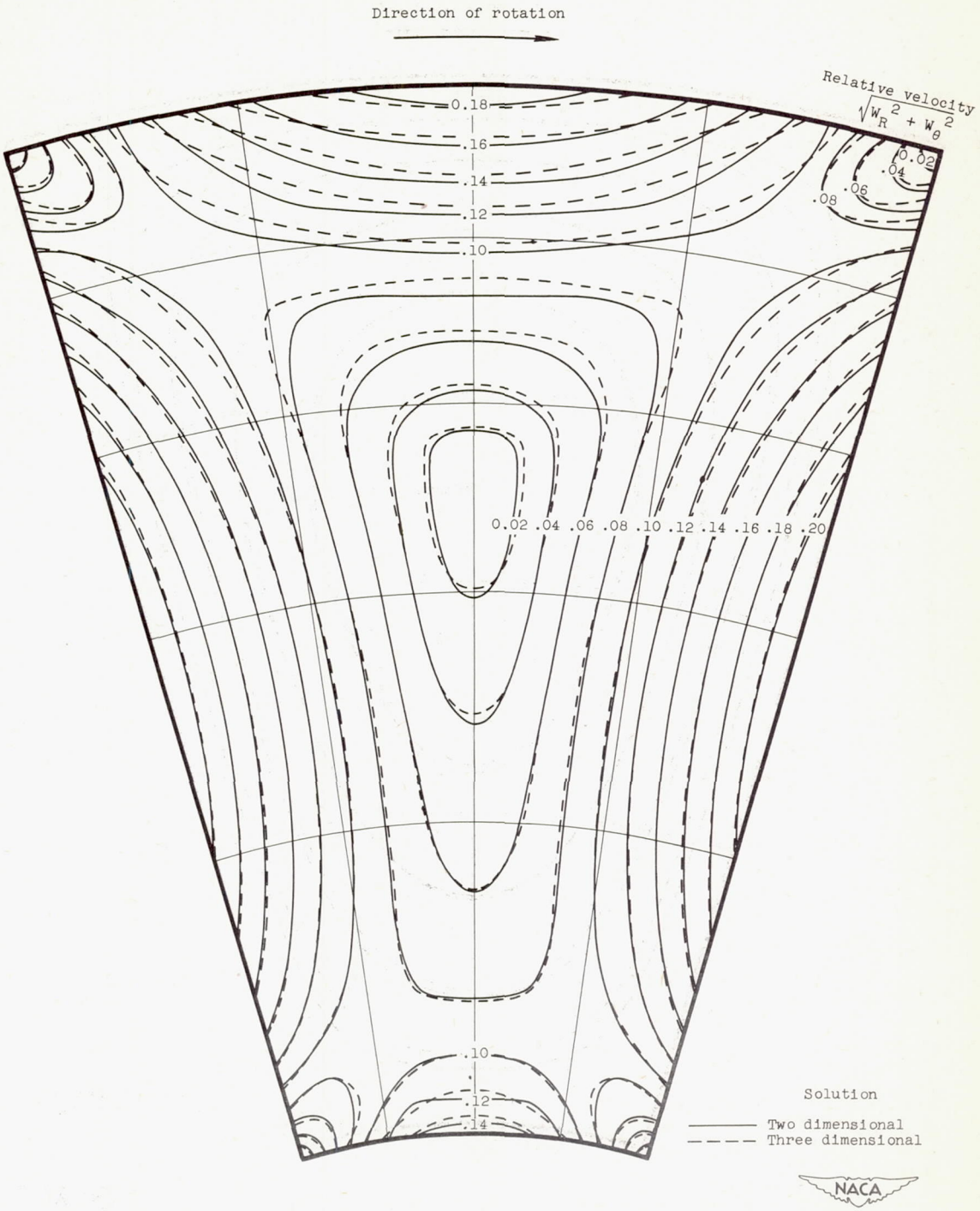

(b) Lines of constant velocity relative to rotating impeller.

Figure 2. - Concluded. Comparison of results obtained from two- and three-dimensional solutions. Plane normal to impeller axis in region of uniform axial velocity far upstream.

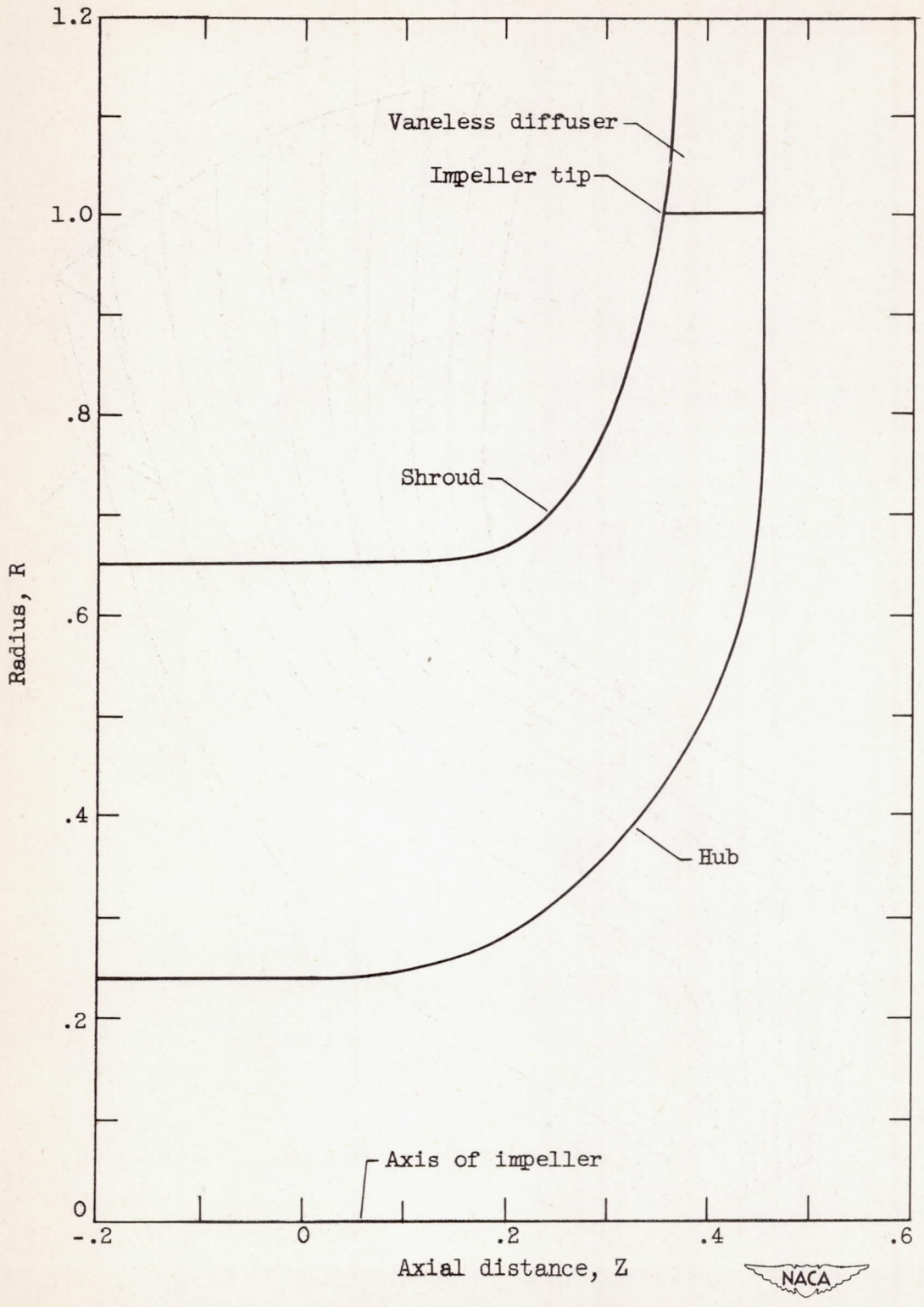

Figure 3. - Hub-shroud dimensions of impeller for numerical examples. Vaneless diffuser; straight impeller blades extended far upstream parallel with axis of impeller.

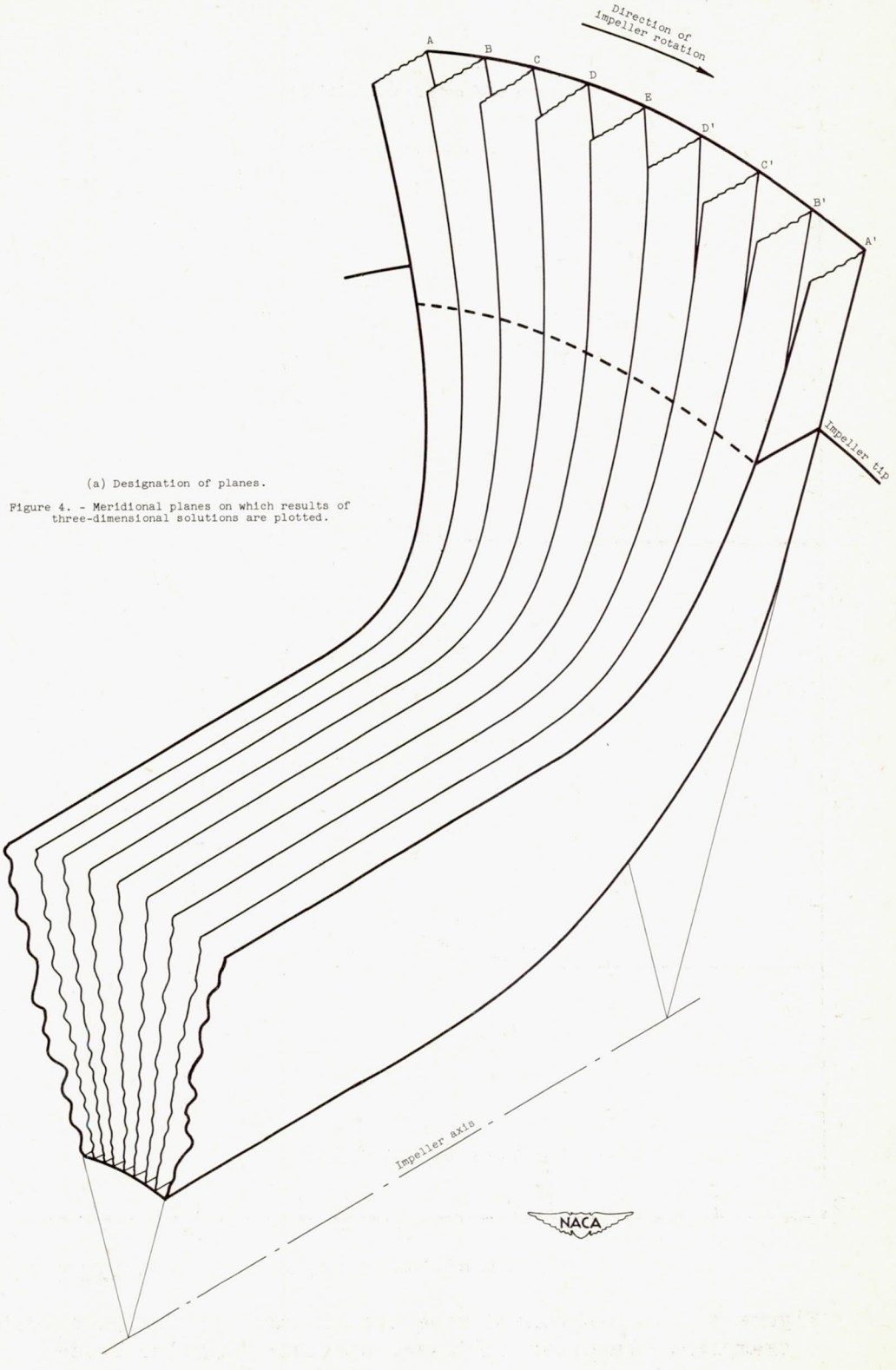

(a) Designation of planes.

Figure 4. - Meridional planes on which results of three-dimensional solutions are plotted.

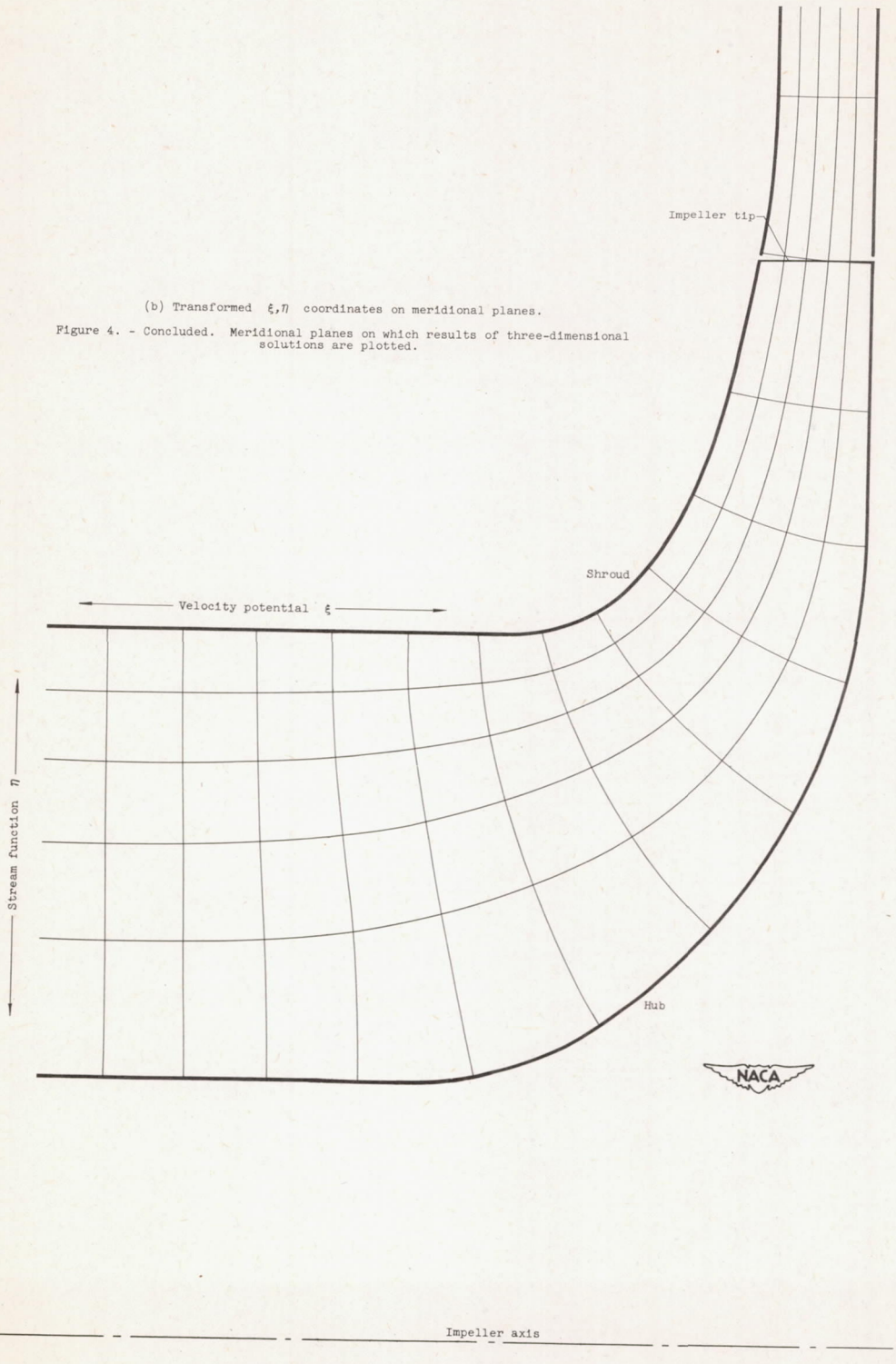

(b) Transformed ξ,η coordinates on meridional planes.

Figure 4. - Concluded. Meridional planes on which results of three-dimensional solutions are plotted.

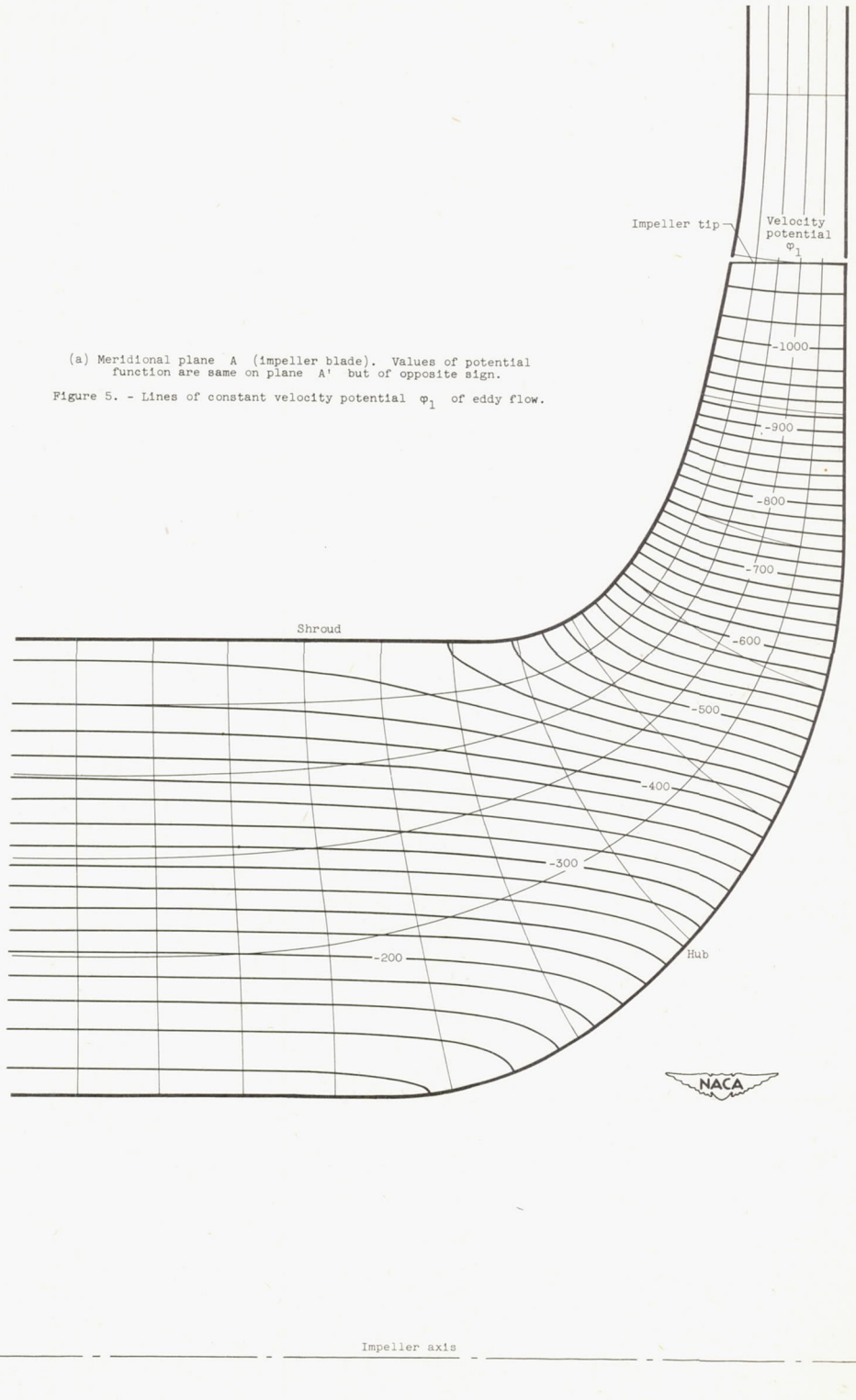

(a) Meridional plane A (impeller blade). Values of potential function are same on plane A' but of opposite sign.

Figure 5. - Lines of constant velocity potential φ_1 of eddy flow.

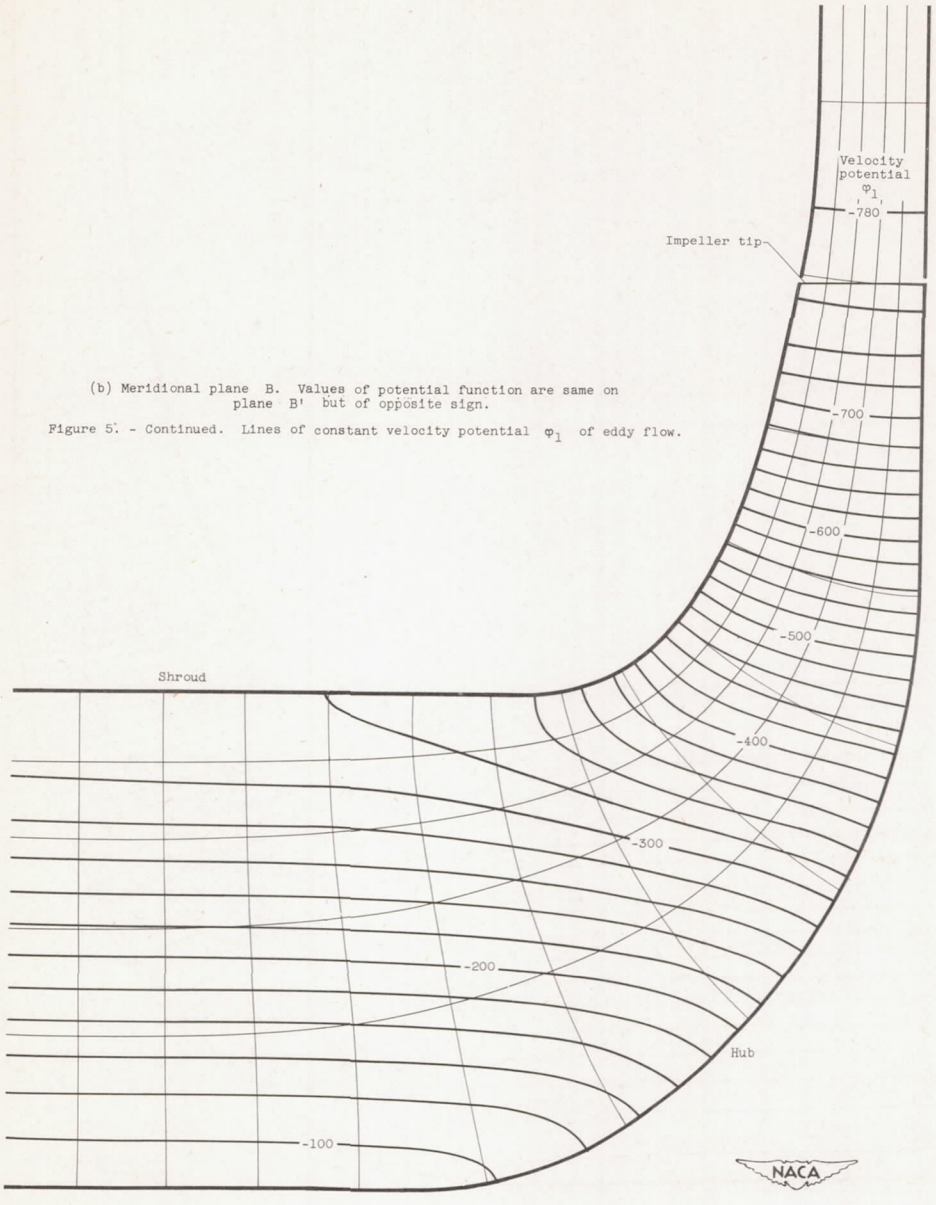

(b) Meridional plane B. Values of potential function are same on plane B' but of opposite sign.

Figure 5. - Continued. Lines of constant velocity potential φ_1 of eddy flow.

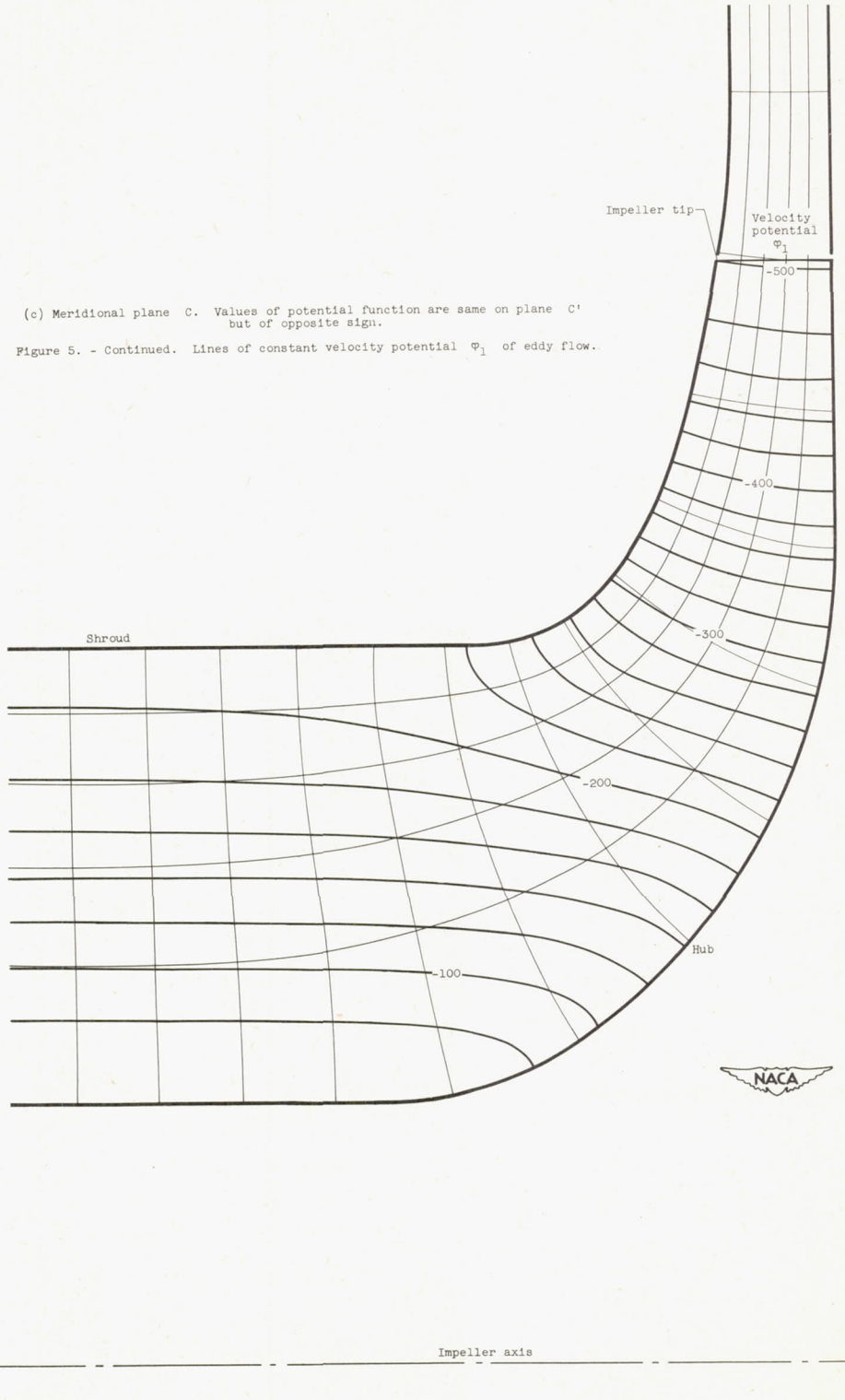

(c) Meridional plane C. Values of potential function are same on plane C' but of opposite sign.

Figure 5. - Continued. Lines of constant velocity potential Φ_1 of eddy flow.

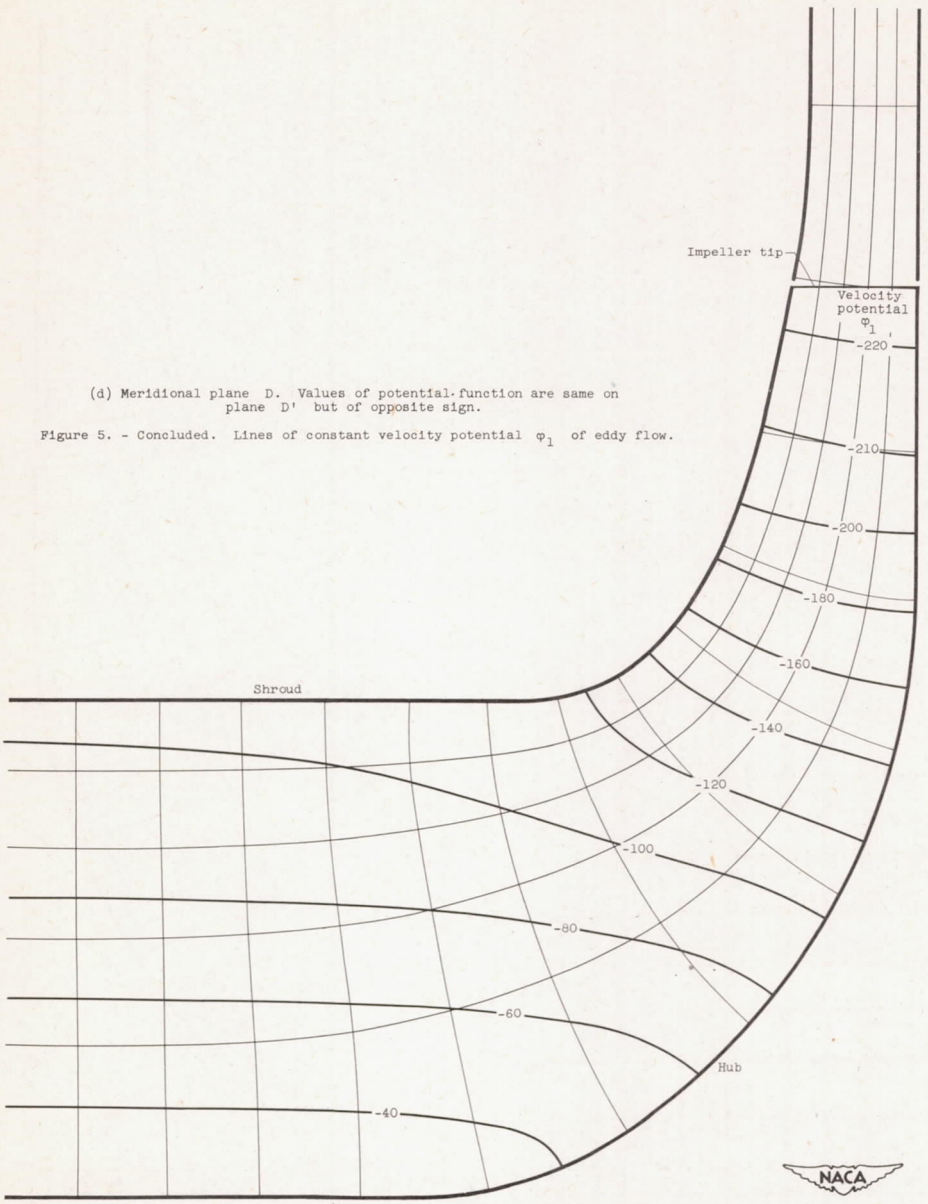

(d) Meridional plane D. Values of potential function are same on plane D' but of opposite sign.

Figure 5. - Concluded. Lines of constant velocity potential φ_1 of eddy flow.

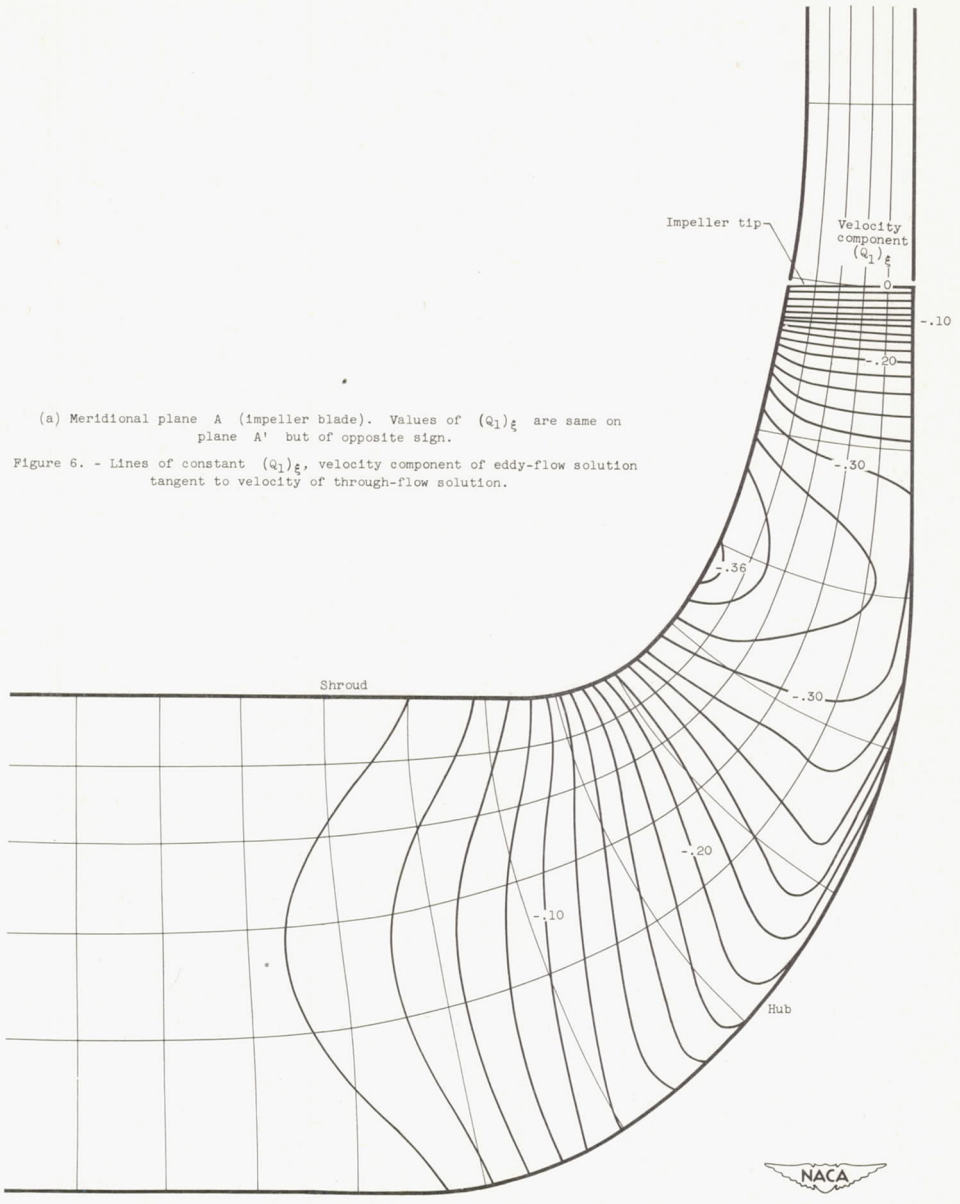

(a) Meridional plane A (impeller blade). Values of $(Q_1)_\xi$ are same on plane A' but of opposite sign.

Figure 6. - Lines of constant $(Q_1)_\xi$, velocity component of eddy-flow solution tangent to velocity of through-flow solution.

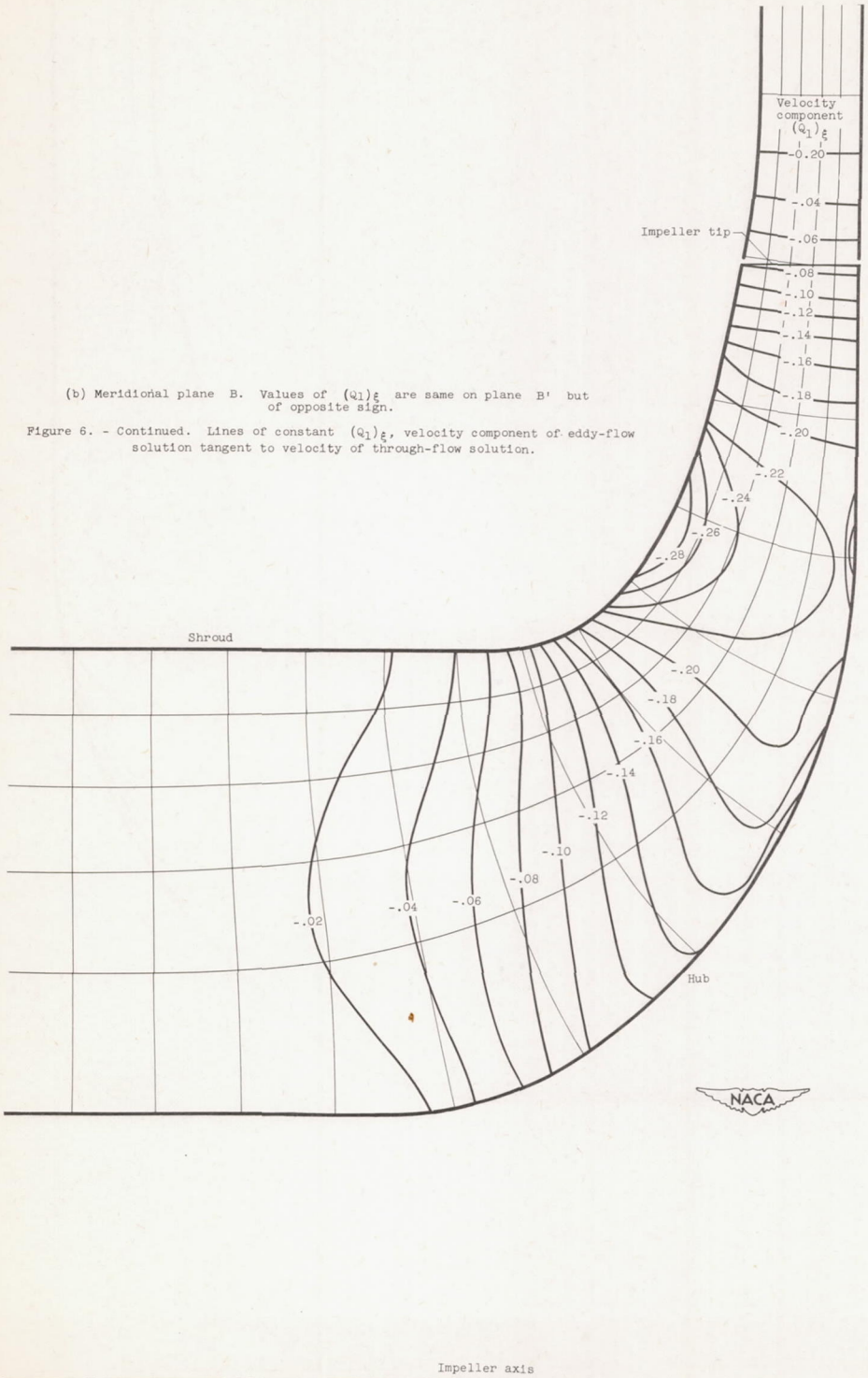

(b) Meridional plane B. Values of $(Q_1)_\xi$ are same on plane B' but of opposite sign.

Figure 6. - Continued. Lines of constant $(Q_1)_\xi$, velocity component of eddy-flow solution tangent to velocity of through-flow solution.

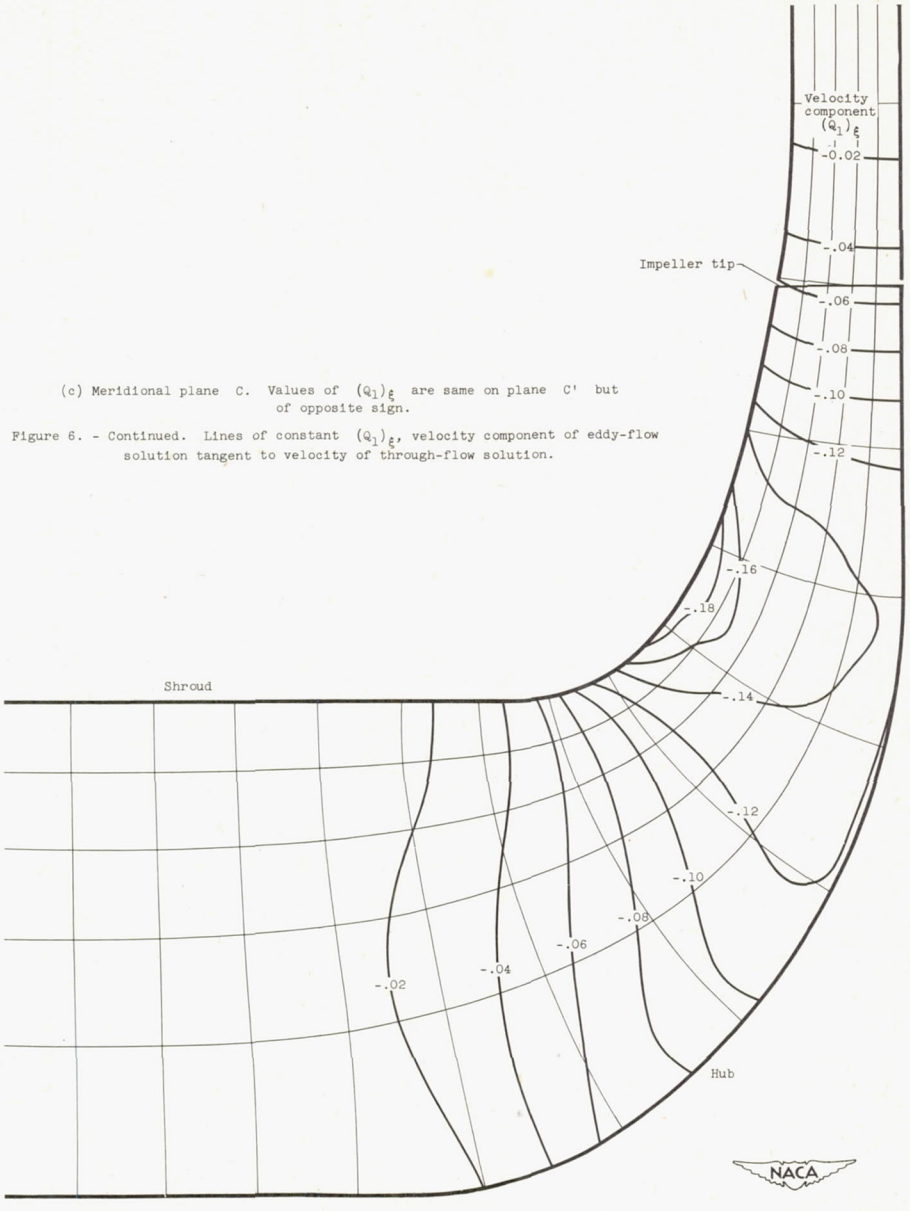

(c) Meridional plane C. Values of $(Q_1)_\xi$ are same on plane C' but of opposite sign.

Figure 6. - Continued. Lines of constant $(Q_1)_\xi$, velocity component of eddy-flow solution tangent to velocity of through-flow solution.

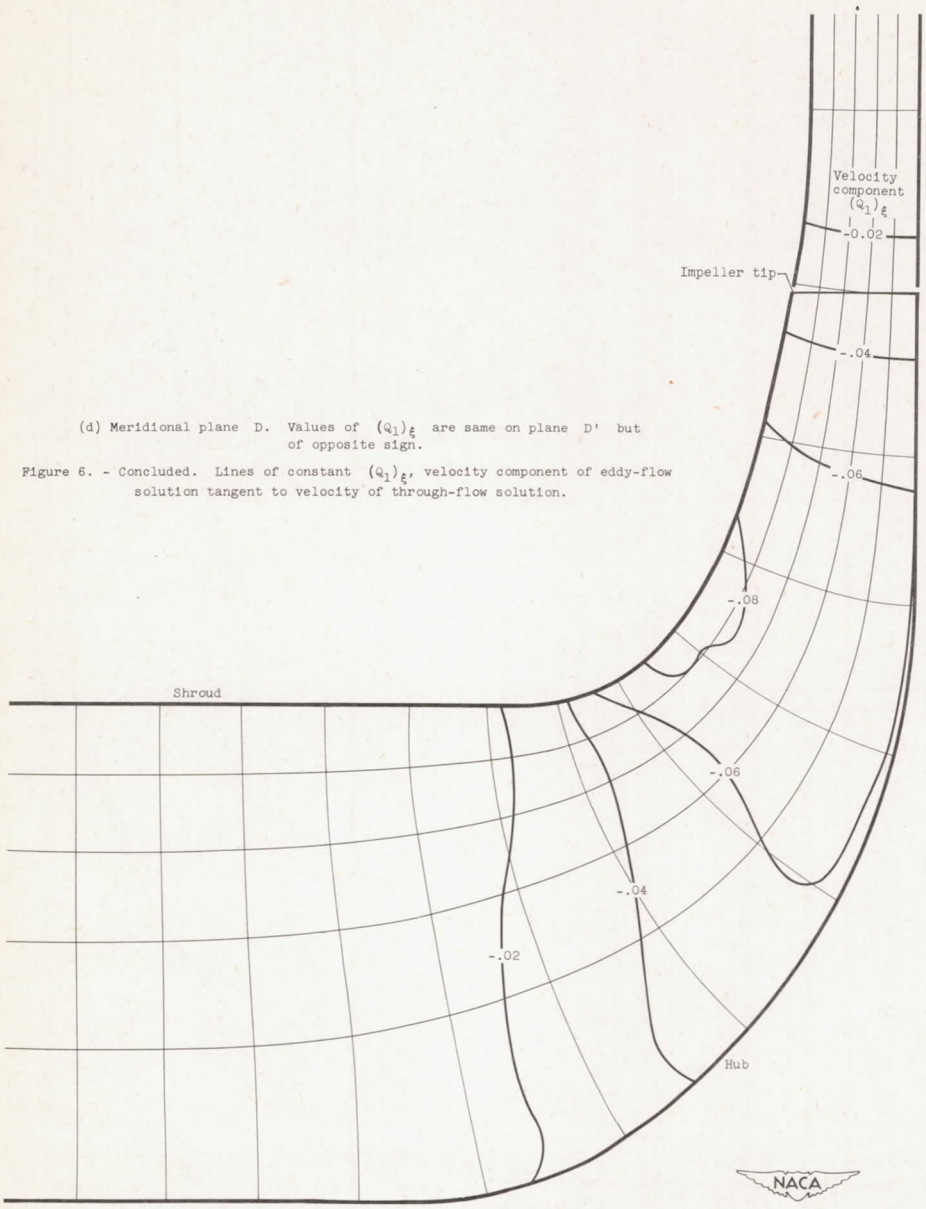

(d) Meridional plane D. Values of $(Q_1)_\xi$ are same on plane D' but of opposite sign.

Figure 6. - Concluded. Lines of constant $(Q_1)_\xi$, velocity component of eddy-flow solution tangent to velocity of through-flow solution.

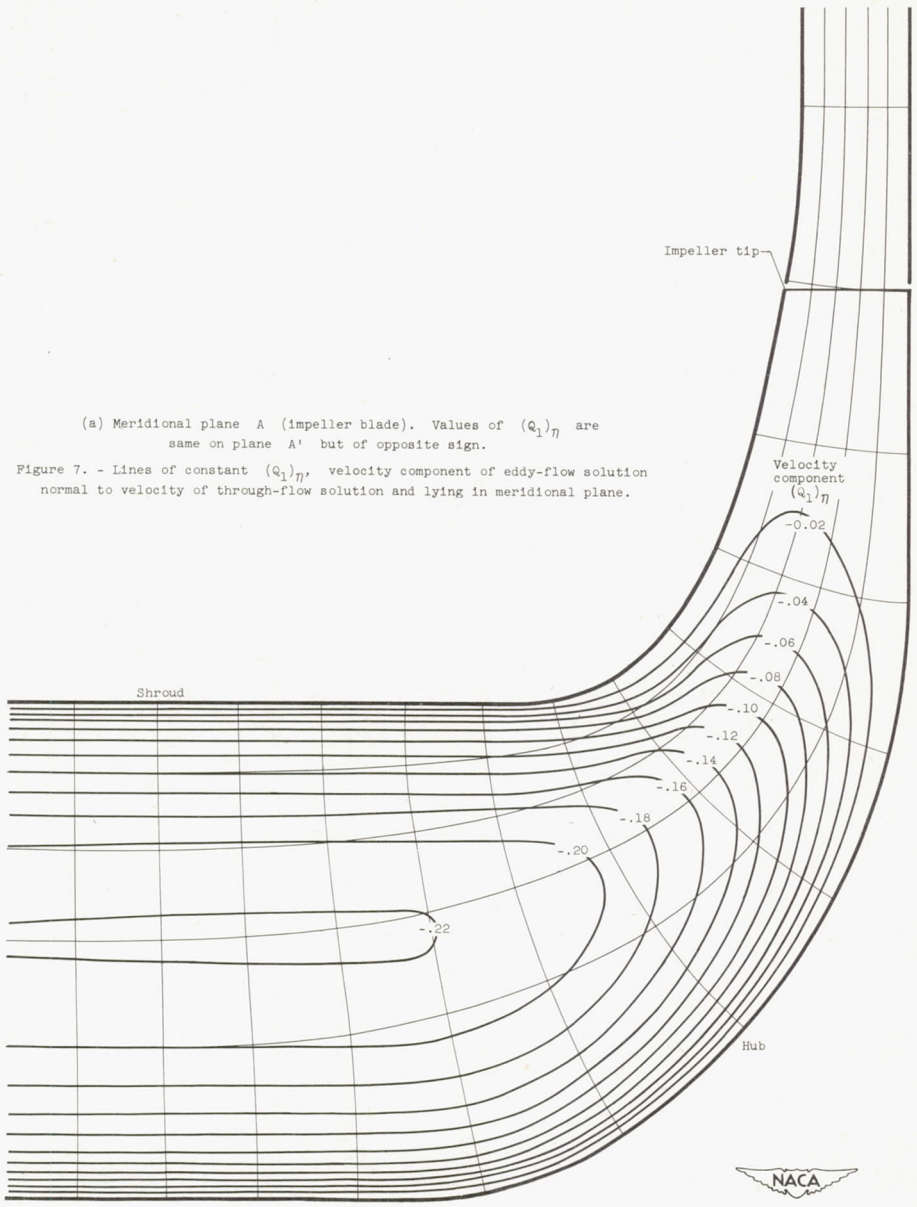

(a) Meridional plane A (impeller blade). Values of $(Q_1)_\eta$ are same on plane A' but of opposite sign.

Figure 7. - Lines of constant $(Q_1)_\eta$, velocity component of eddy-flow solution normal to velocity of through-flow solution and lying in meridional plane.

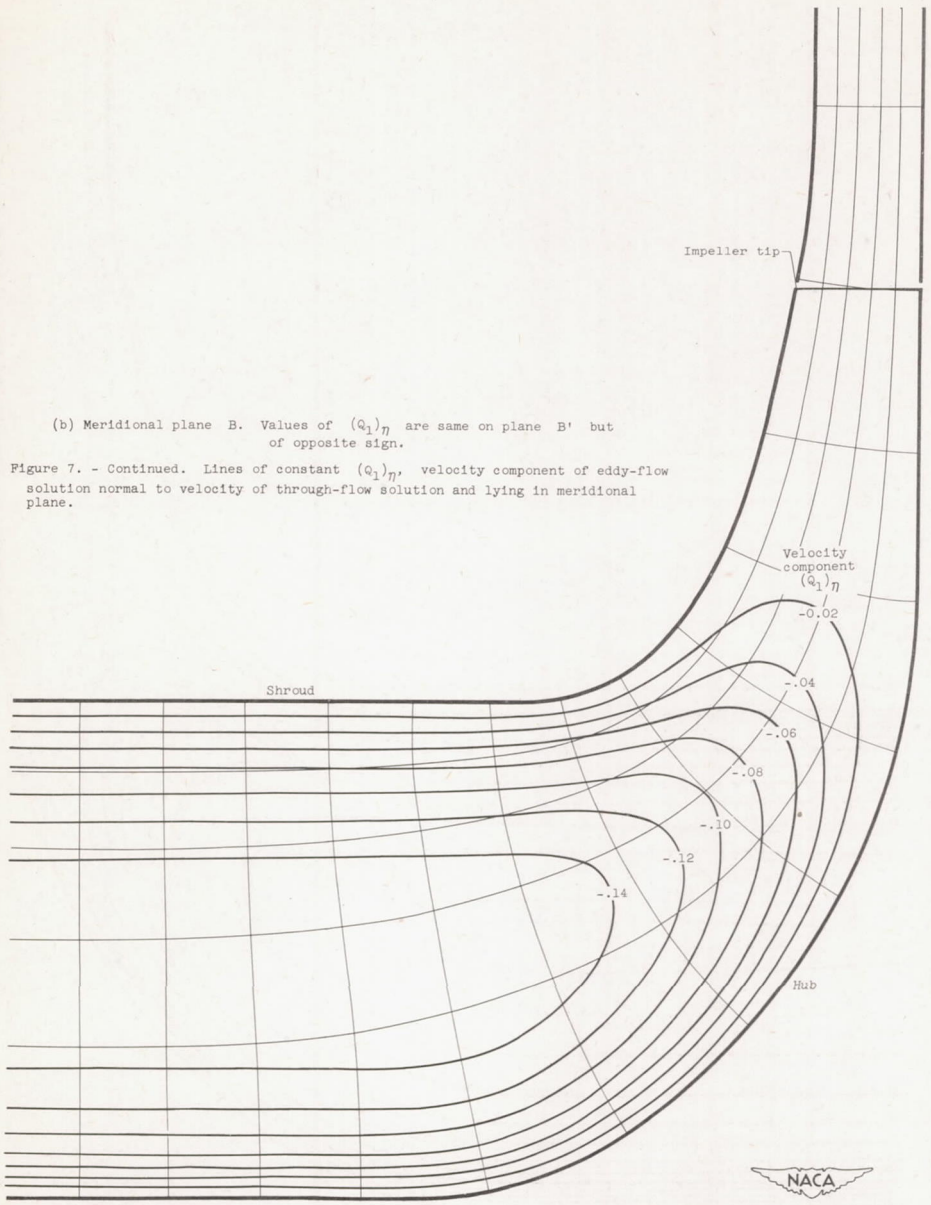

(b) Meridional plane B. Values of $(Q_1)_\eta$ are same on plane B' but of opposite sign.

Figure 7. - Continued. Lines of constant $(Q_1)_\eta$, velocity component of eddy-flow solution normal to velocity of through-flow solution and lying in meridional plane.

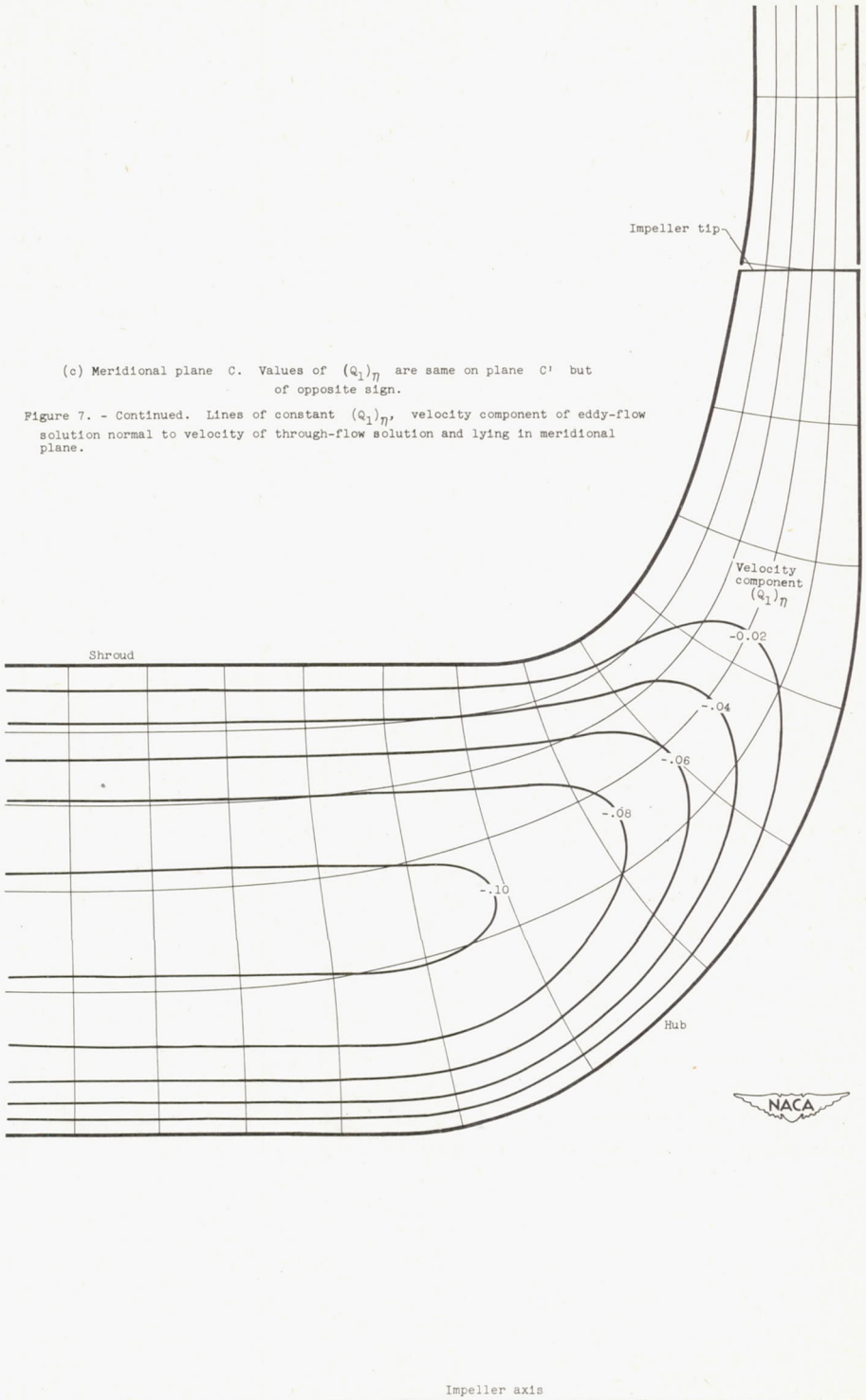

(c) Meridional plane C. Values of $(Q_1)_\eta$ are same on plane C' but of opposite sign.

Figure 7. - Continued. Lines of constant $(Q_1)_\eta$, velocity component of eddy-flow solution normal to velocity of through-flow solution and lying in meridional plane.

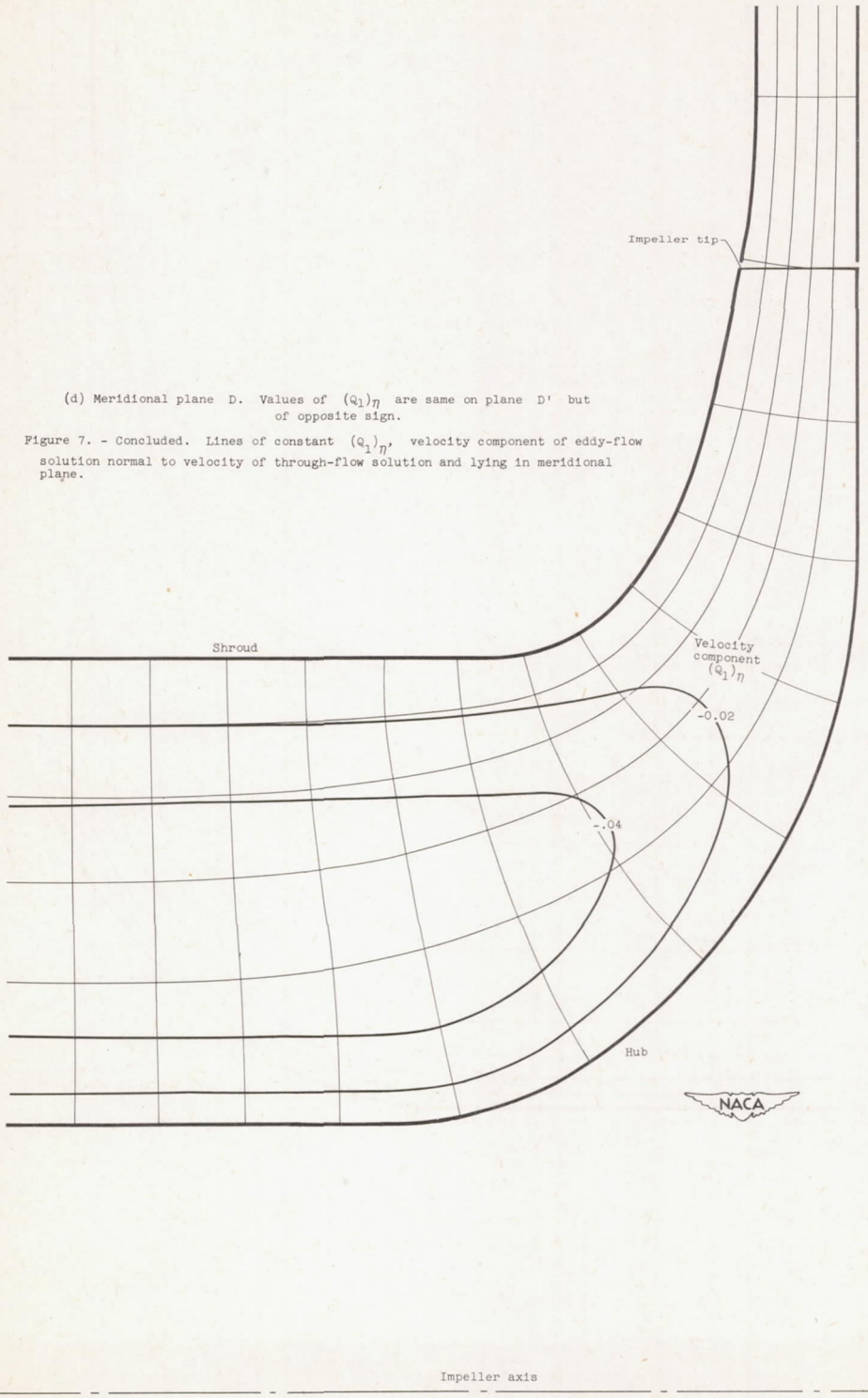

(d) Meridional plane D. Values of $(Q_1)_\eta$ are same on plane D' but of opposite sign.

Figure 7. - Concluded. Lines of constant $(Q_1)_\eta$, velocity component of eddy-flow solution normal to velocity of through-flow solution and lying in meridional plane.

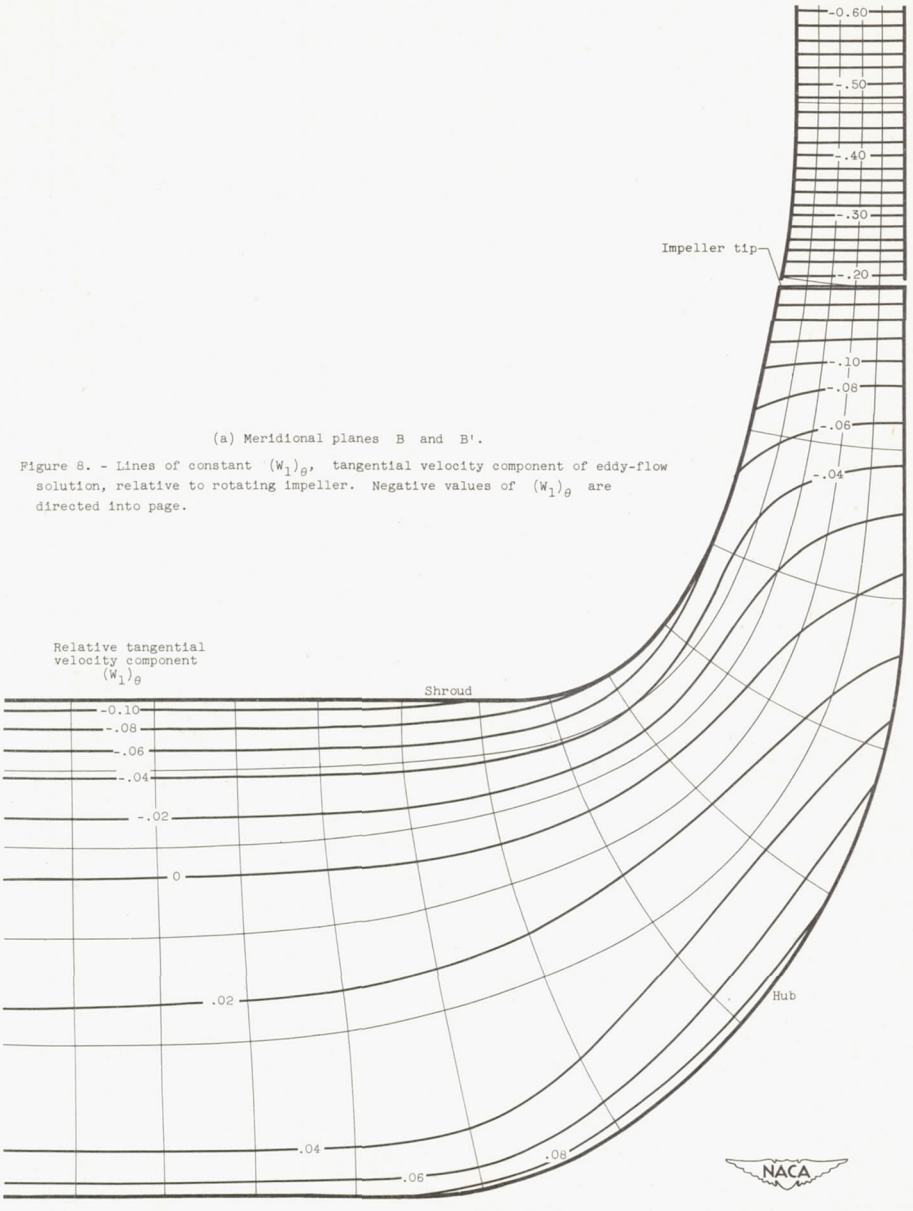

(a) Meridional planes B and B'.

Figure 8. - Lines of constant $(W_1)_\theta$, tangential velocity component of eddy-flow solution, relative to rotating impeller. Negative values of $(W_1)_\theta$ are directed into page.

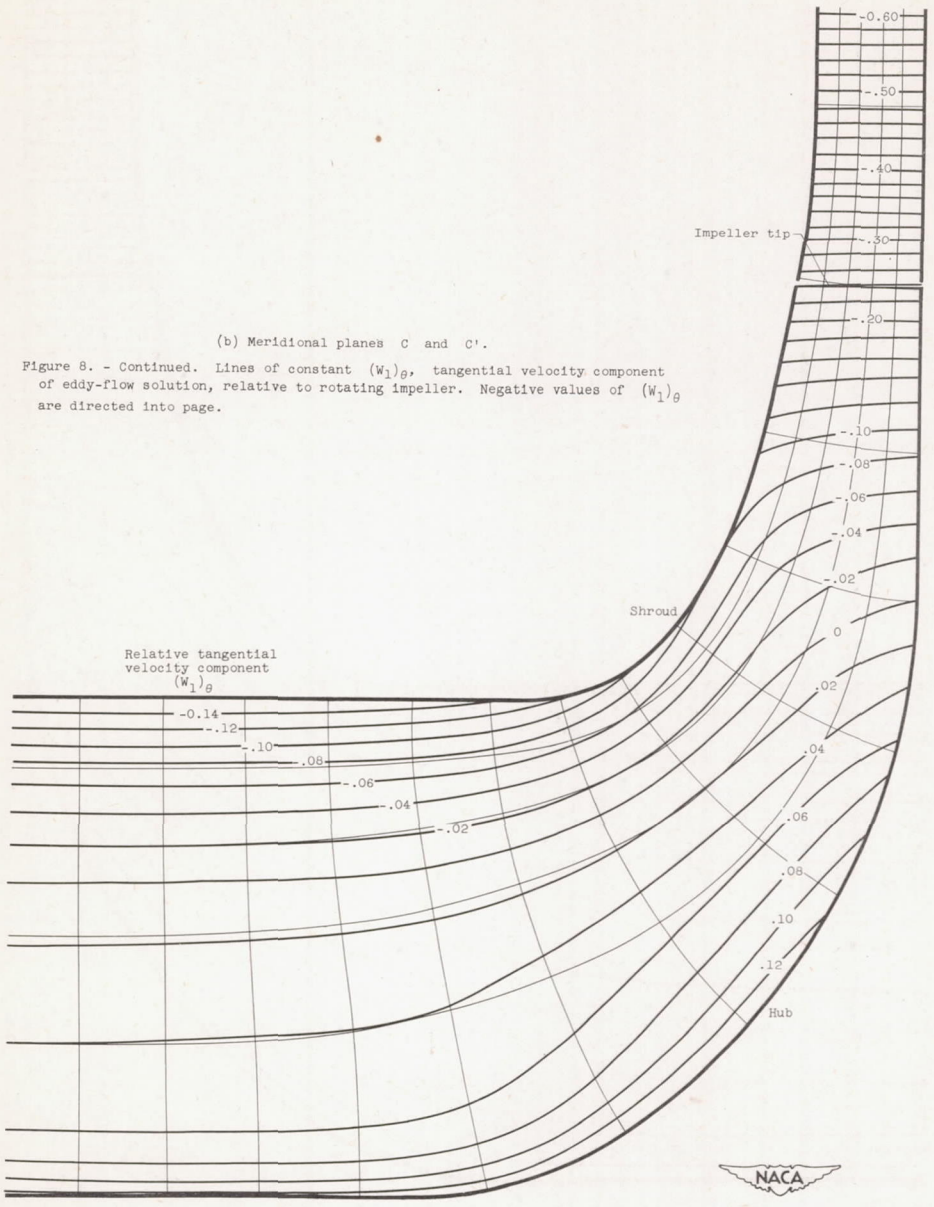

(b) Meridional planes C and C'.

Figure 8. - Continued. Lines of constant $(W_1)_\theta$, tangential velocity component of eddy-flow solution, relative to rotating impeller. Negative values of $(W_1)_\theta$ are directed into page.

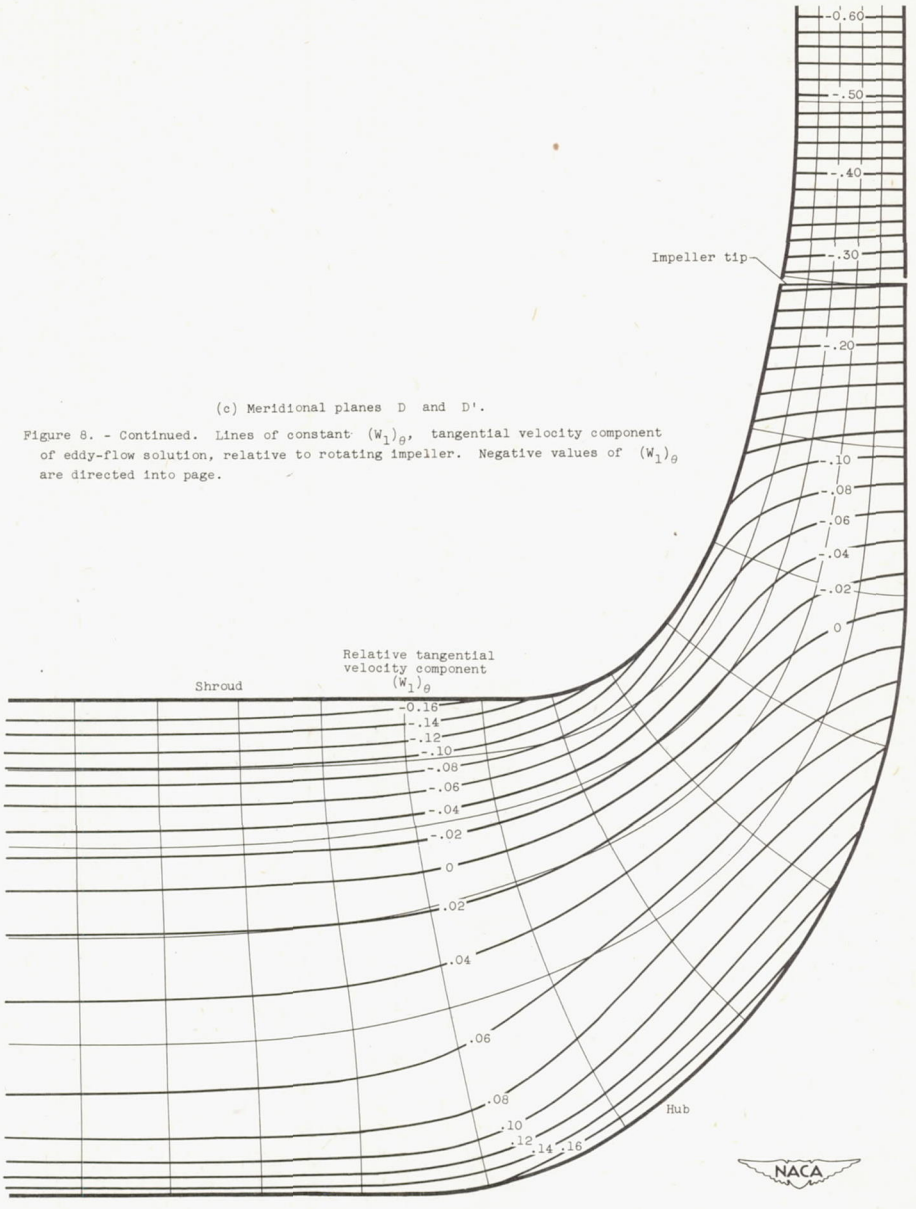

(c) Meridional planes D and D'.

Figure 8. - Continued. Lines of constant $(W_1)_\theta$, tangential velocity component of eddy-flow solution, relative to rotating impeller. Negative values of $(W_1)_\theta$ are directed into page.

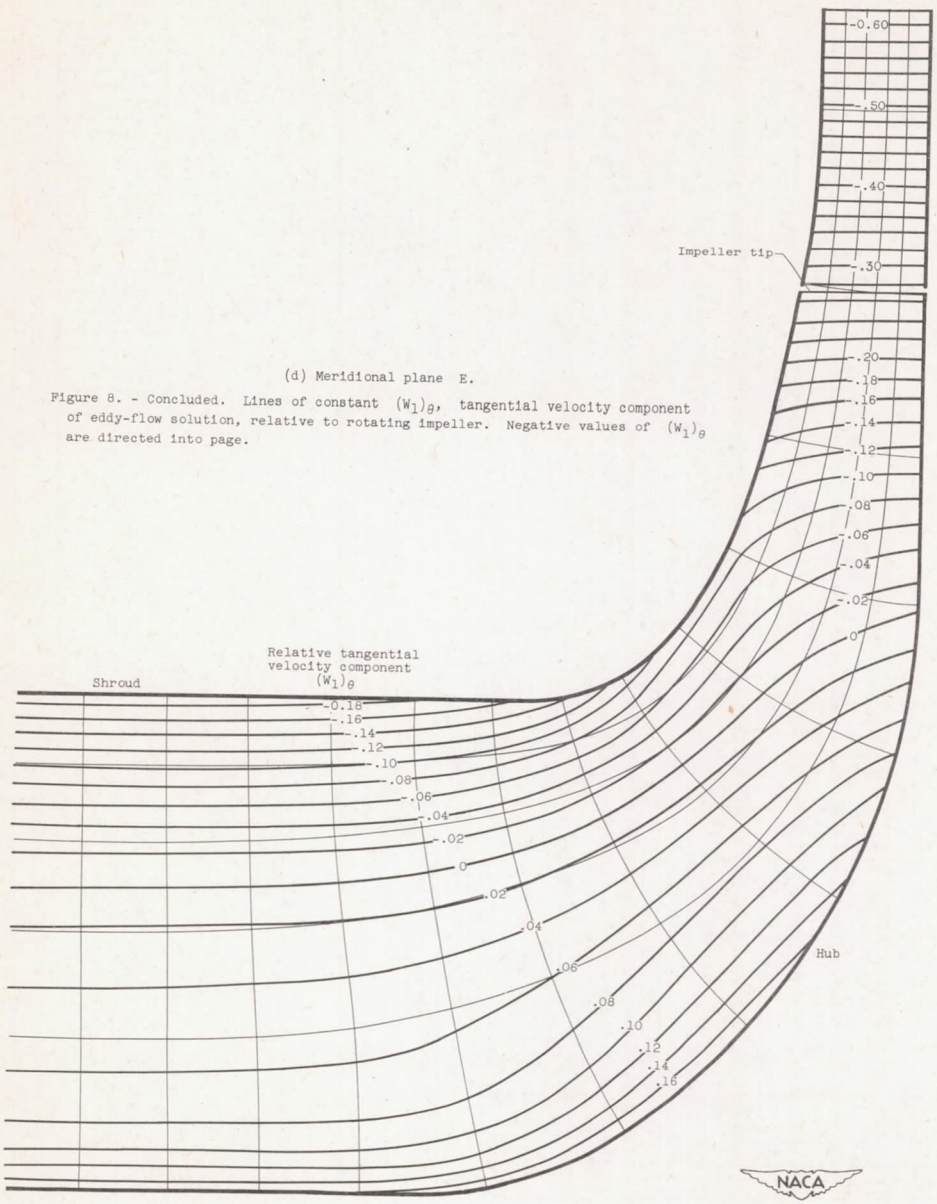

(d) Meridional plane E.

Figure 8. - Concluded. Lines of constant $(W_1)_\theta$, tangential velocity component of eddy-flow solution, relative to rotating impeller. Negative values of $(W_1)_\theta$ are directed into page.

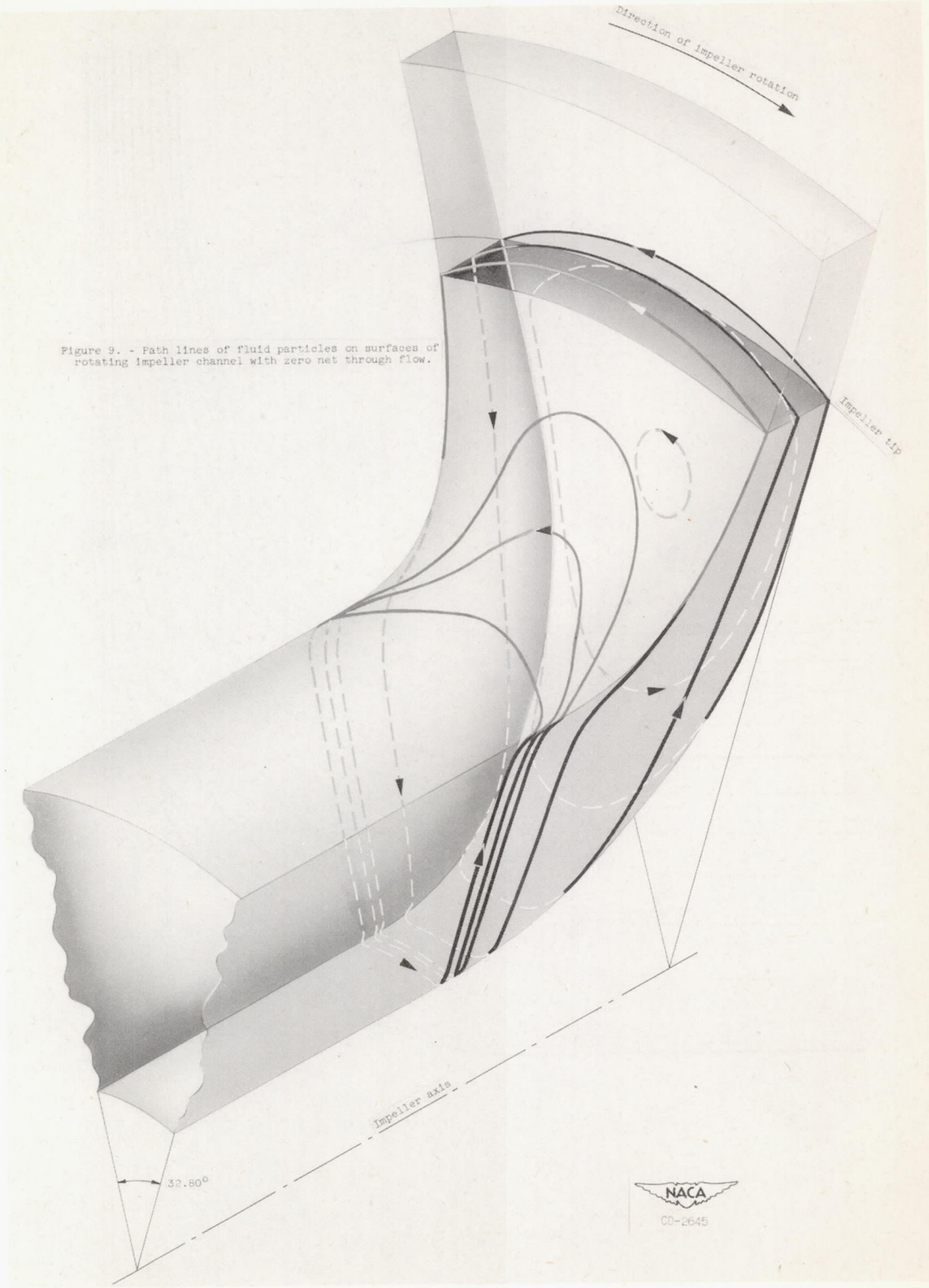

Figure 9. - Path lines of fluid particles on surfaces of rotating impeller channel with zero net through flow.

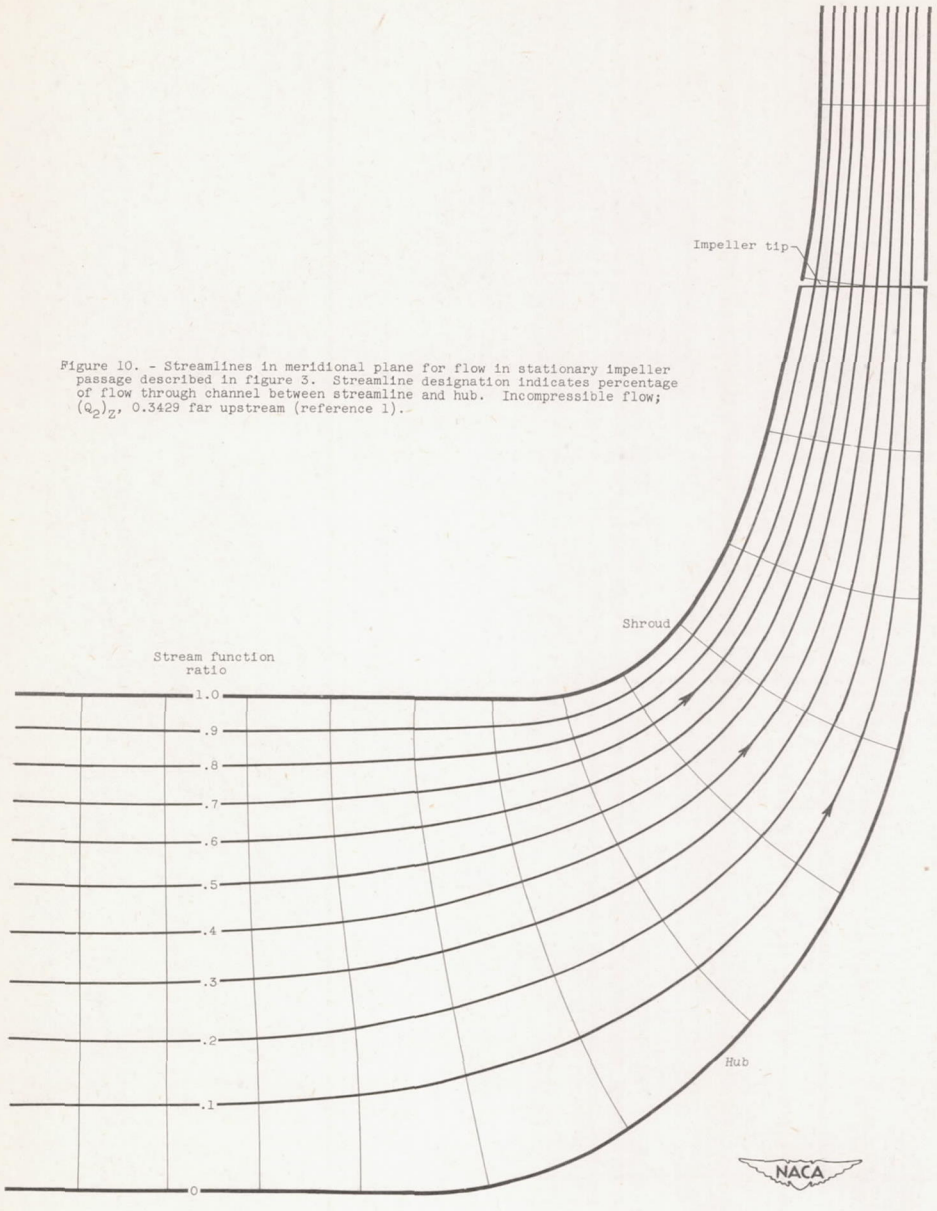

Figure 10. - Streamlines in meridional plane for flow in stationary impeller passage described in figure 3. Streamline designation indicates percentage of flow through channel between streamline and hub. Incompressible flow; $(Q_2)_Z$, 0.3429 far upstream (reference 1).

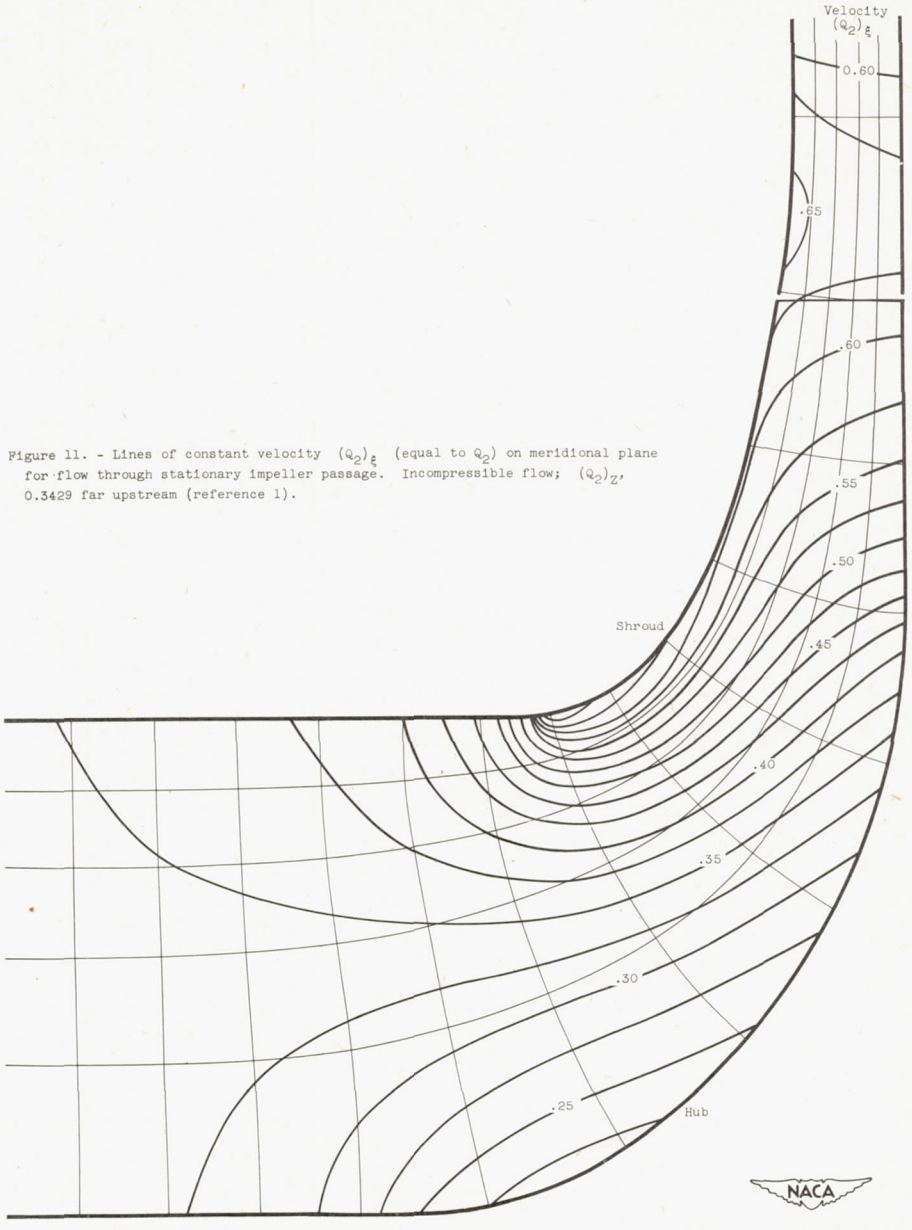

Figure 11. - Lines of constant velocity $(Q_2)_\xi$ (equal to Q_2) on meridional plane for flow through stationary impeller passage. Incompressible flow; $(Q_2)_Z$, 0.3429 far upstream (reference 1).

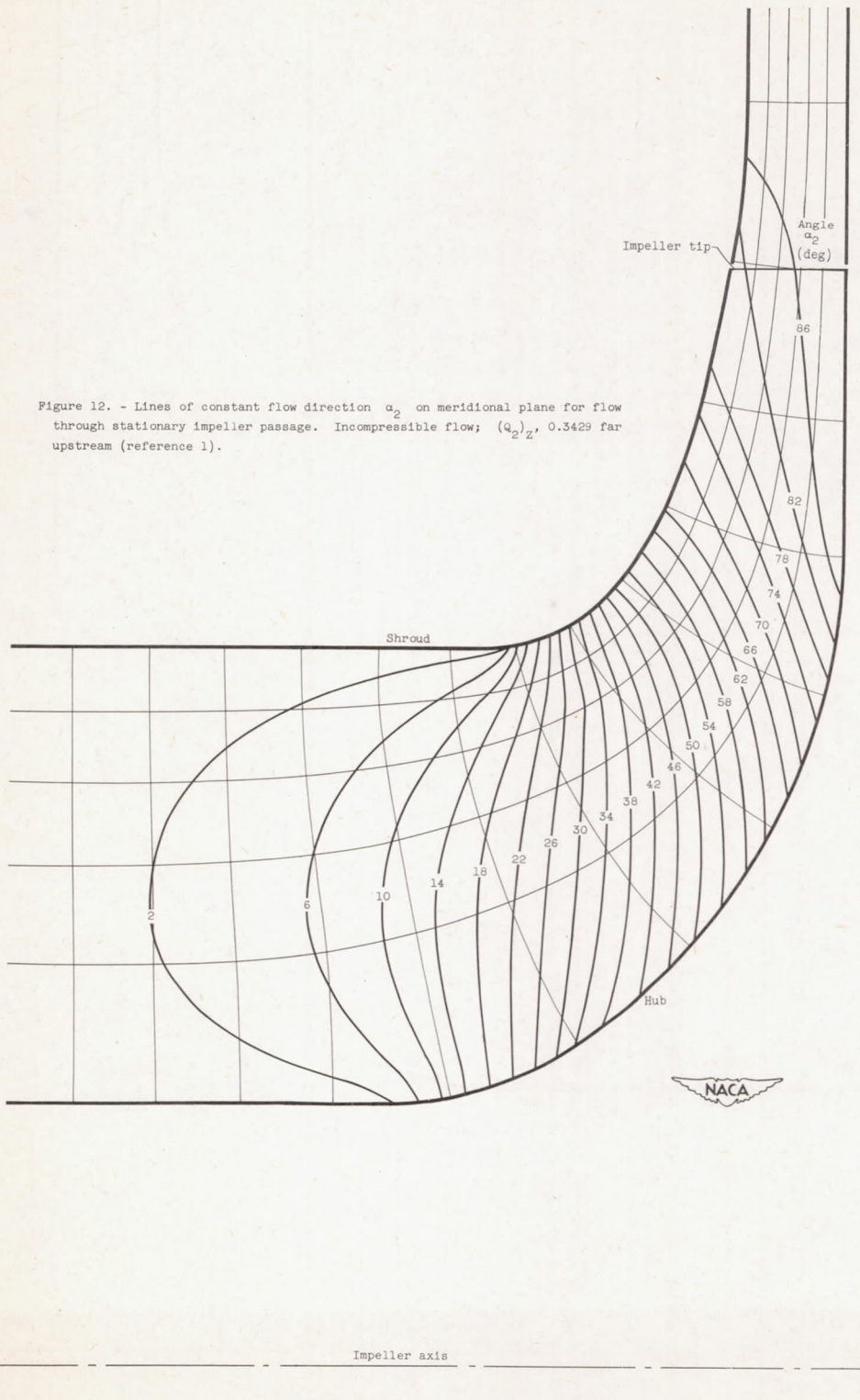

Figure 12. - Lines of constant flow direction α_2 on meridional plane for flow through stationary impeller passage. Incompressible flow; $(Q_2)_Z$, 0.3429 far upstream (reference 1).

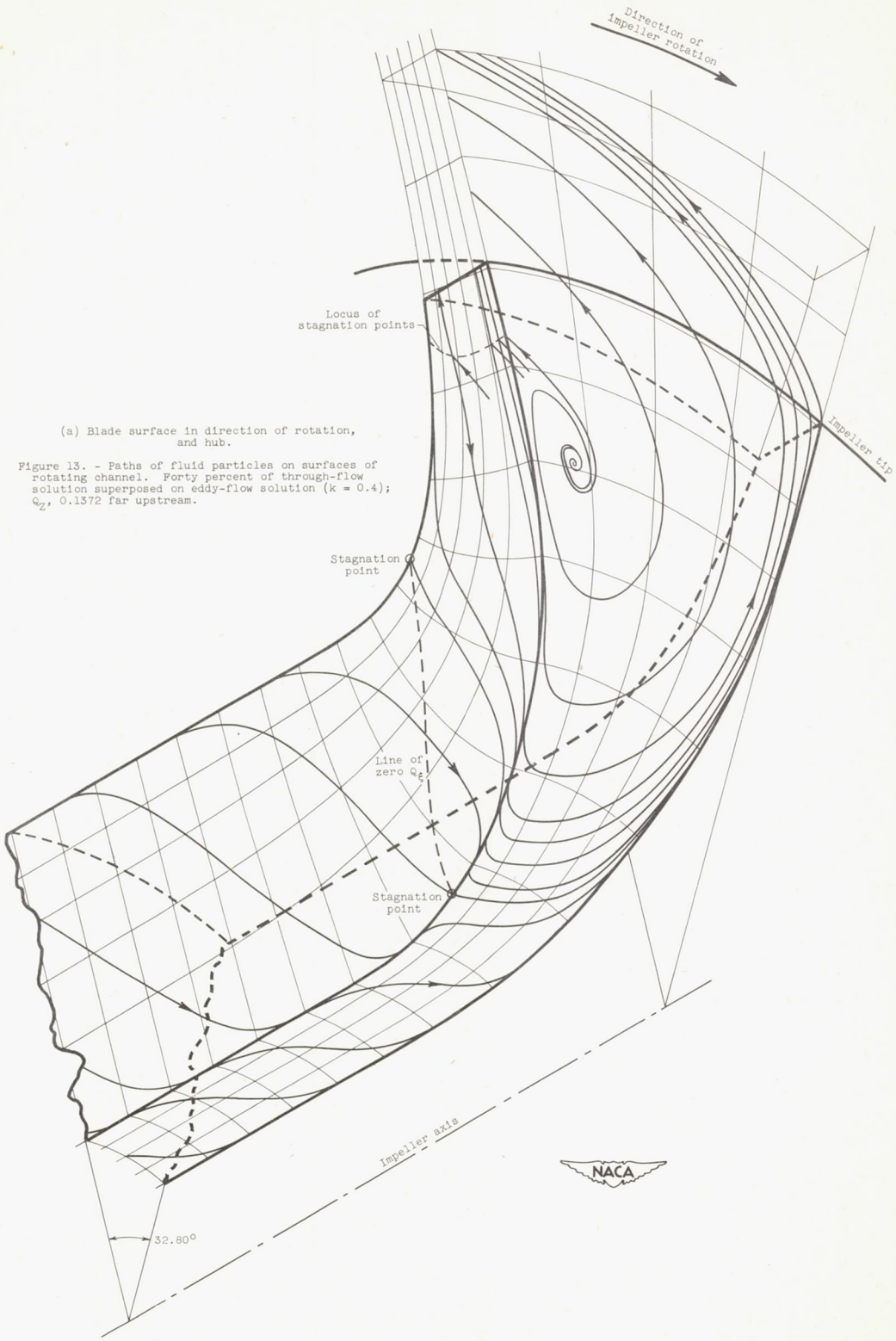

(a) Blade surface in direction of rotation, and hub.

Figure 13. - Paths of fluid particles on surfaces of rotating channel. Forty percent of through-flow solution superposed on eddy-flow solution ($k = 0.4$); Q_z, 0.1372 far upstream.

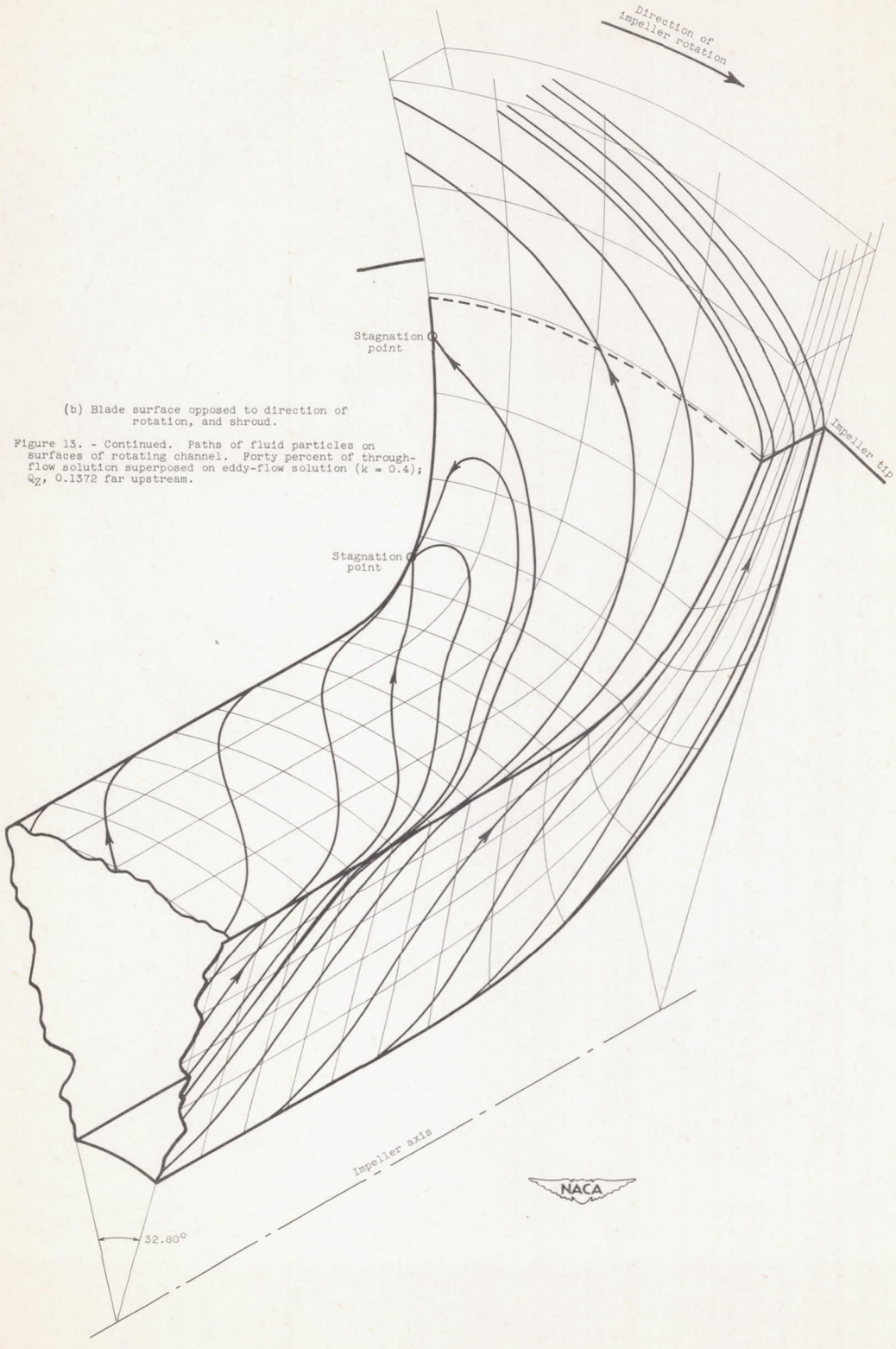

(b) Blade surface opposed to direction of rotation, and shroud.

Figure 13. - Continued. Paths of fluid particles on surfaces of rotating channel. Forty percent of through-flow solution superposed on eddy-flow solution ($k = 0.4$); Q_Z, 0.1372 far upstream.

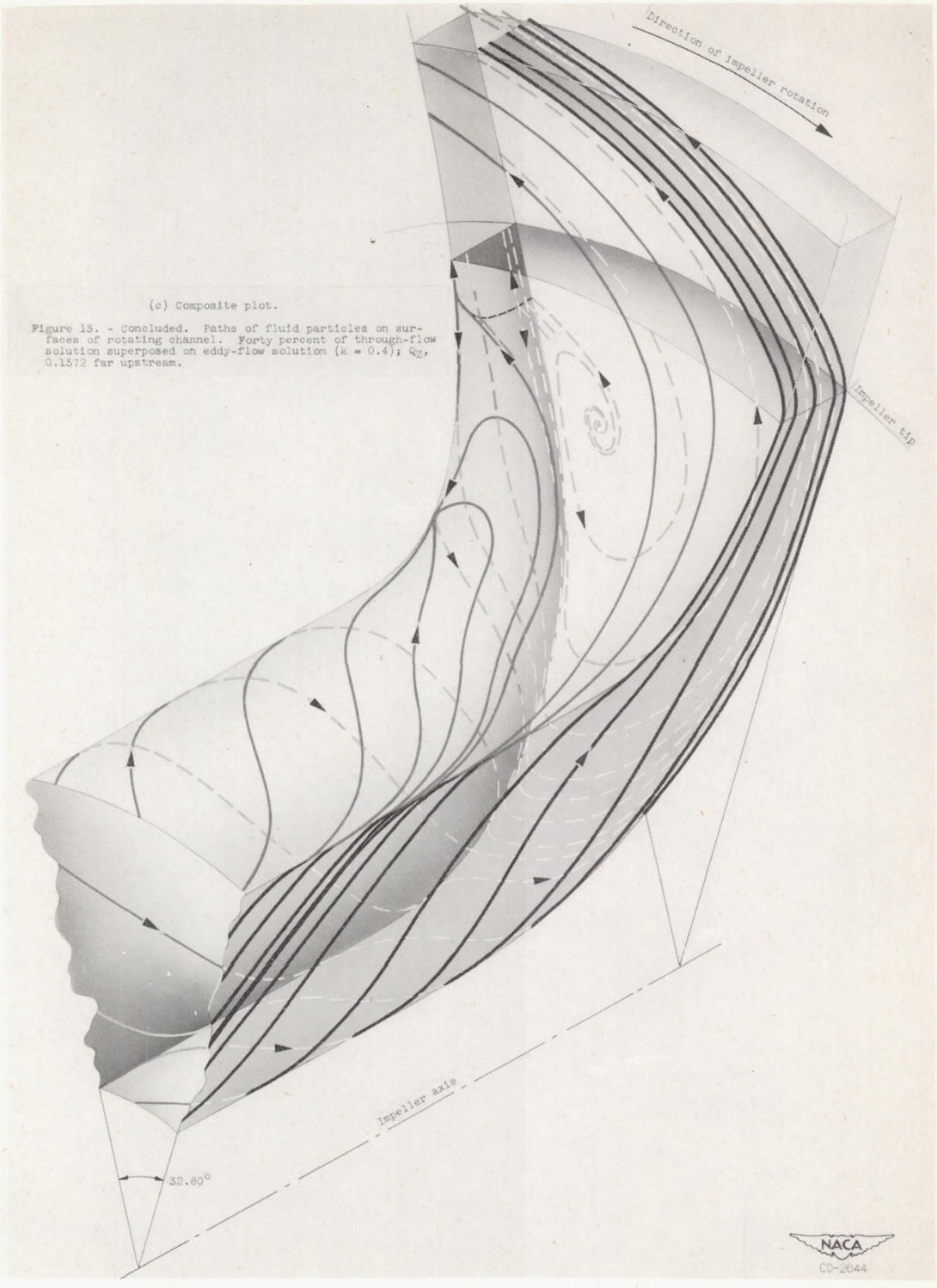

(c) Composite plot.

Figure 13. - Concluded. Paths of fluid particles on surfaces of rotating channel. Forty percent of through-flow solution superposed on eddy-flow solution ($k = 0.4$); Q_Z, 0.1372 far upstream.

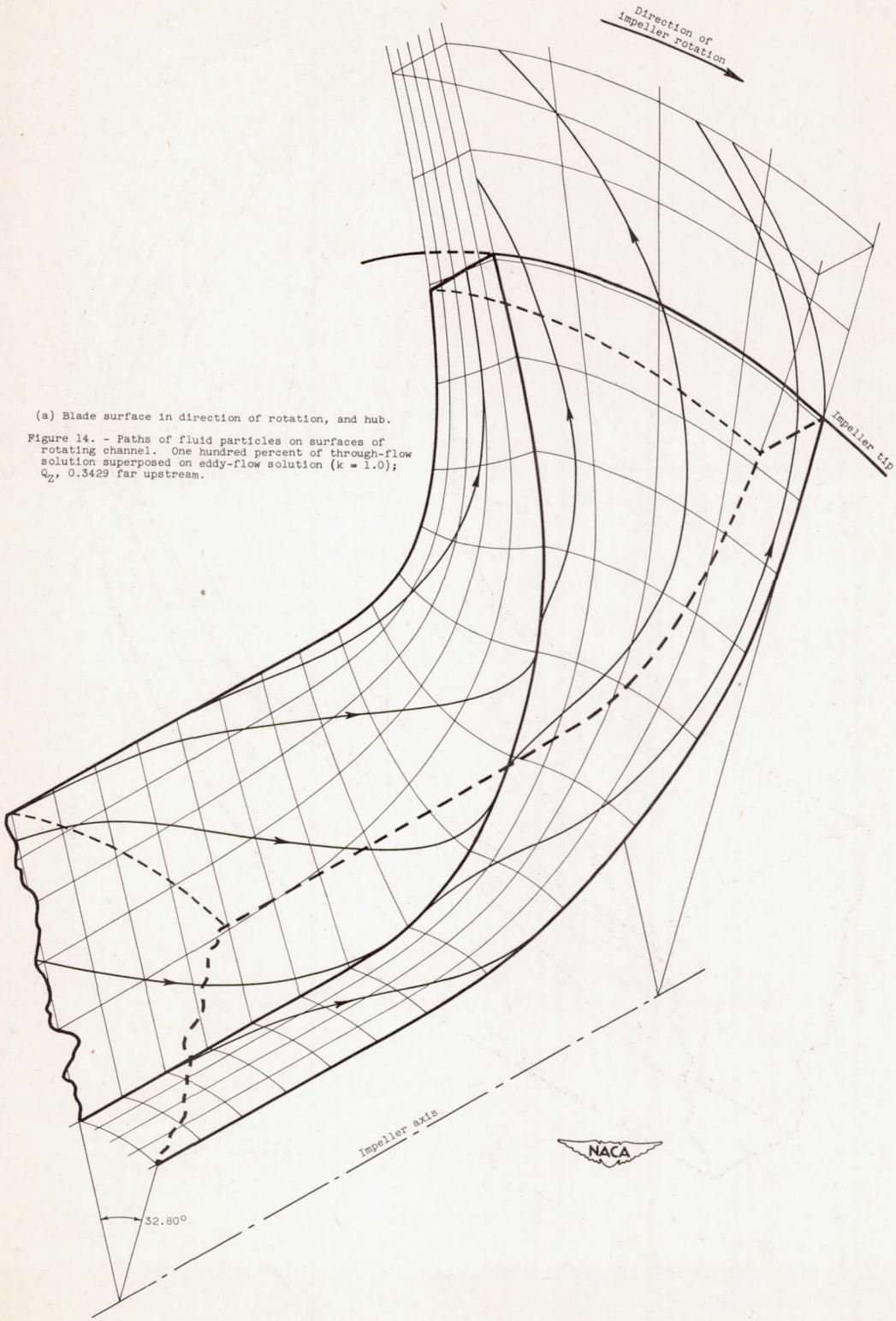

(a) Blade surface in direction of rotation, and hub.

Figure 14. - Paths of fluid particles on surfaces of rotating channel. One hundred percent of through-flow solution superposed on eddy-flow solution (k = 1.0); Q_z, 0.3429 far upstream.

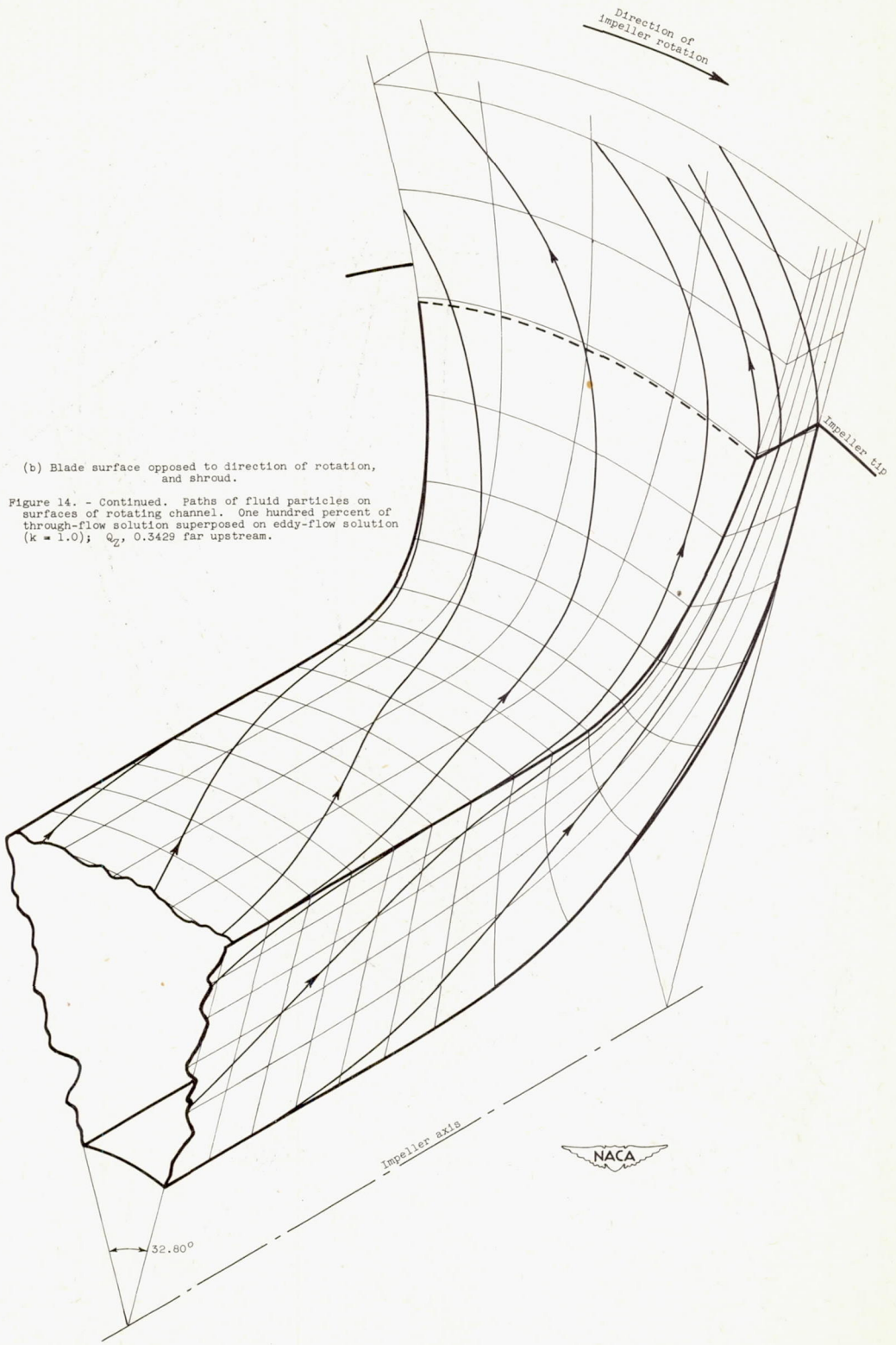

(b) Blade surface opposed to direction of rotation, and shroud.

Figure 14. - Continued. Paths of fluid particles on surfaces of rotating channel. One hundred percent of through-flow solution superposed on eddy-flow solution (k = 1.0); Q_Z, 0.3429 far upstream.

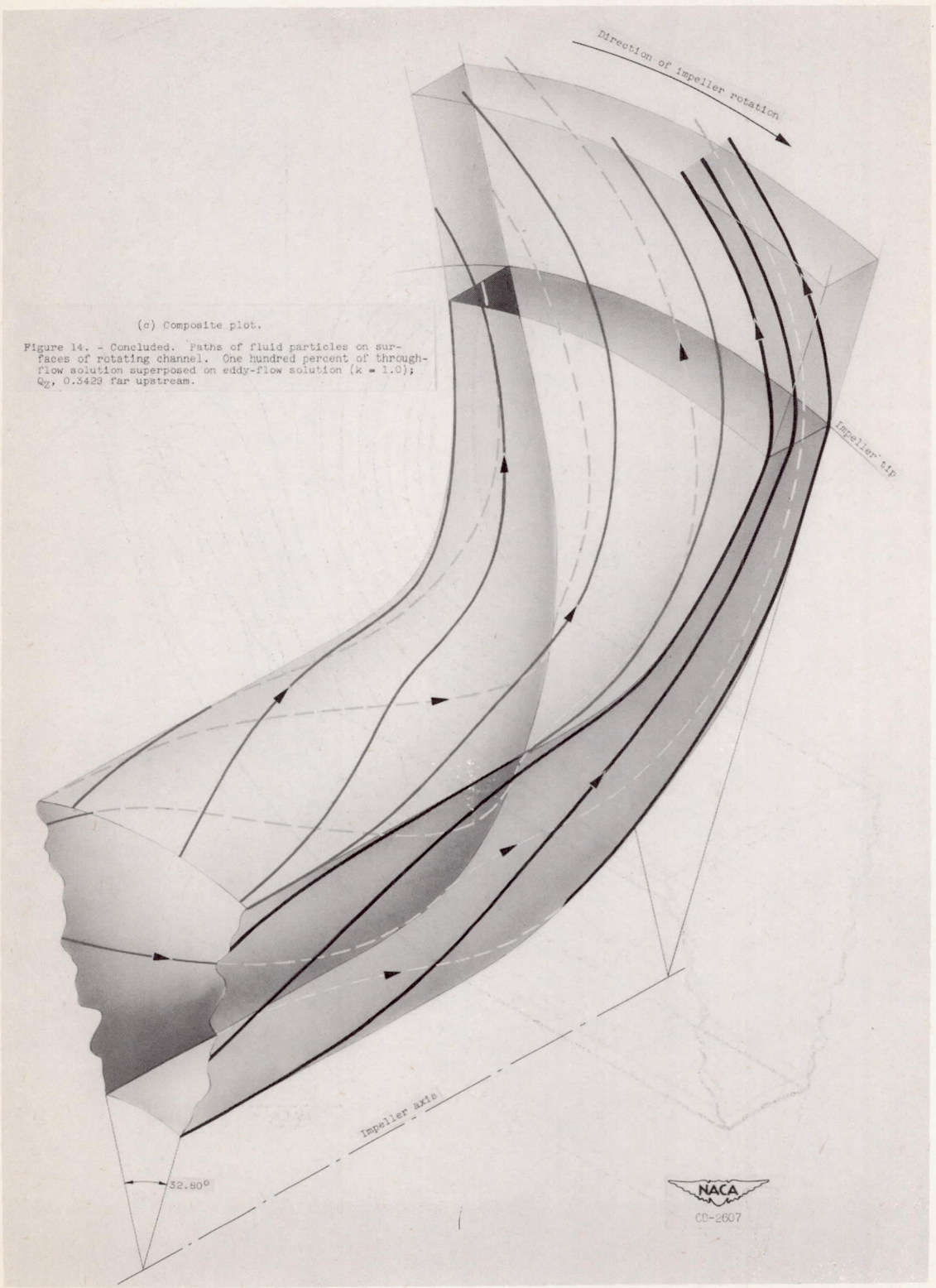

(c) Composite plot.

Figure 14. - Concluded. Paths of fluid particles on surfaces of rotating channel. One hundred percent of through-flow solution superposed on eddy-flow solution ($k = 1.0$); Q_Z, 0.3429 far upstream.

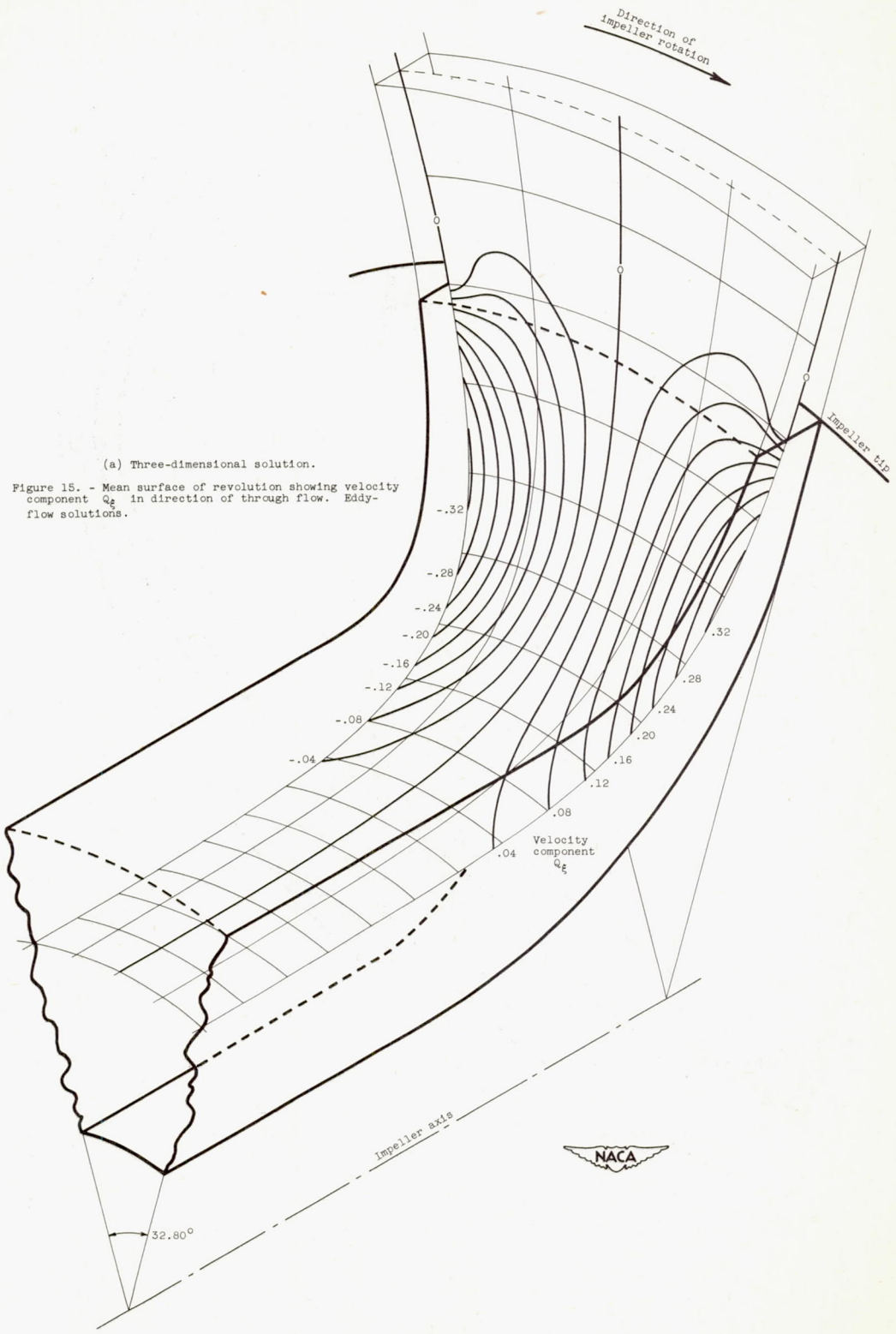

(a) Three-dimensional solution.

Figure 15. - Mean surface of revolution showing velocity component Q_ξ in direction of through flow. Eddy-flow solutions.

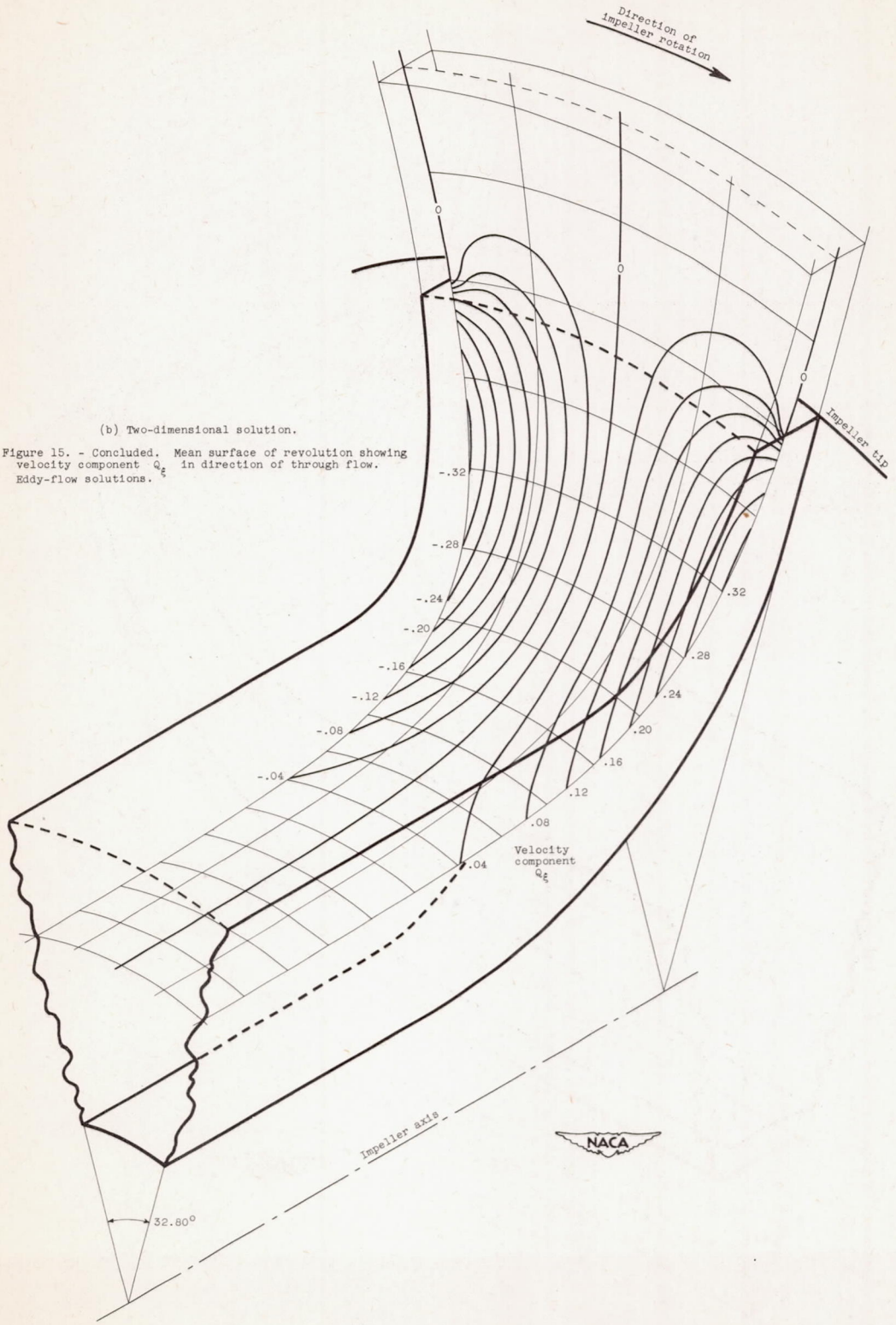

(b) Two-dimensional solution.

Figure 15. - Concluded. Mean surface of revolution showing velocity component Q_ξ in direction of through flow. Eddy-flow solutions.

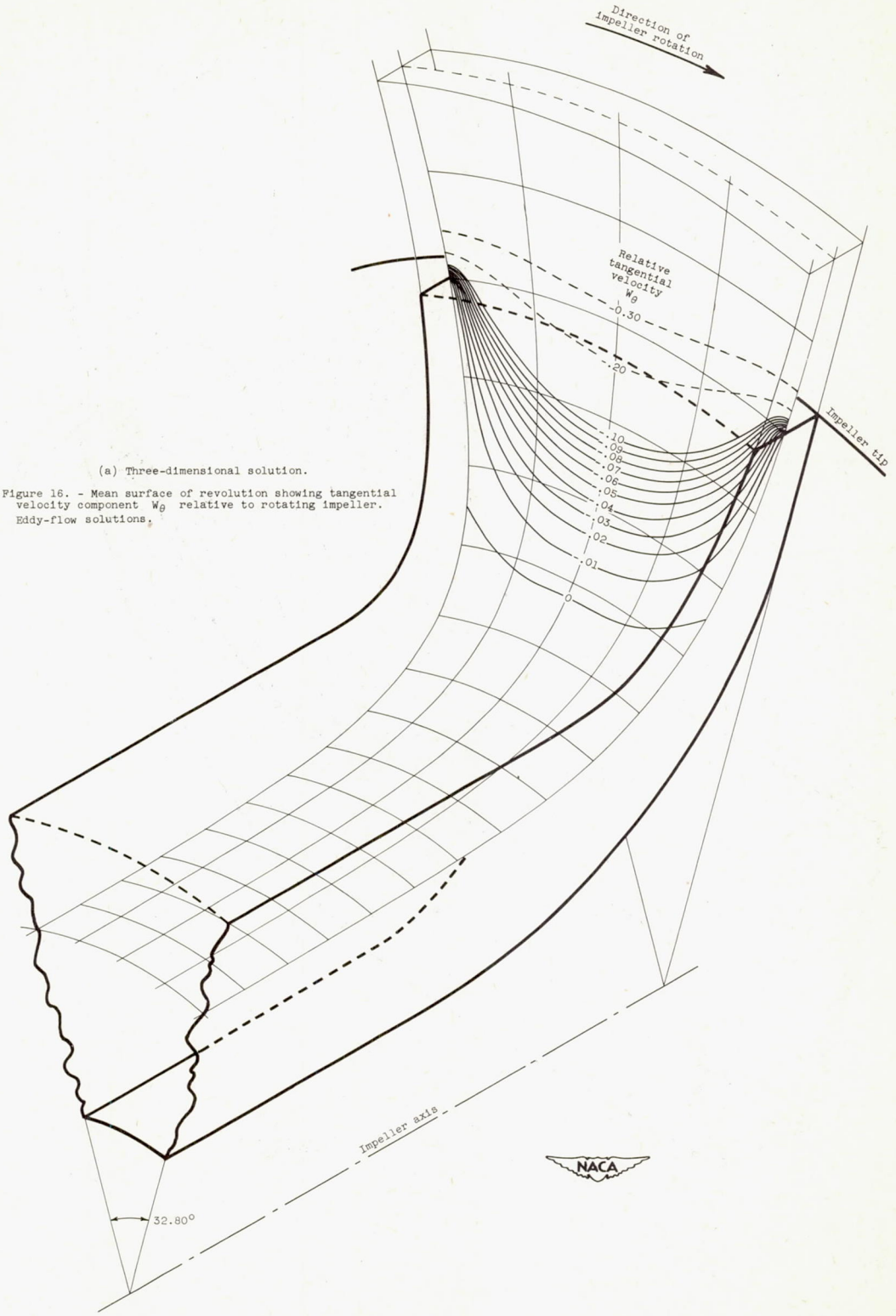

(a) Three-dimensional solution.

Figure 16. - Mean surface of revolution showing tangential velocity component W_θ relative to rotating impeller. Eddy-flow solutions.

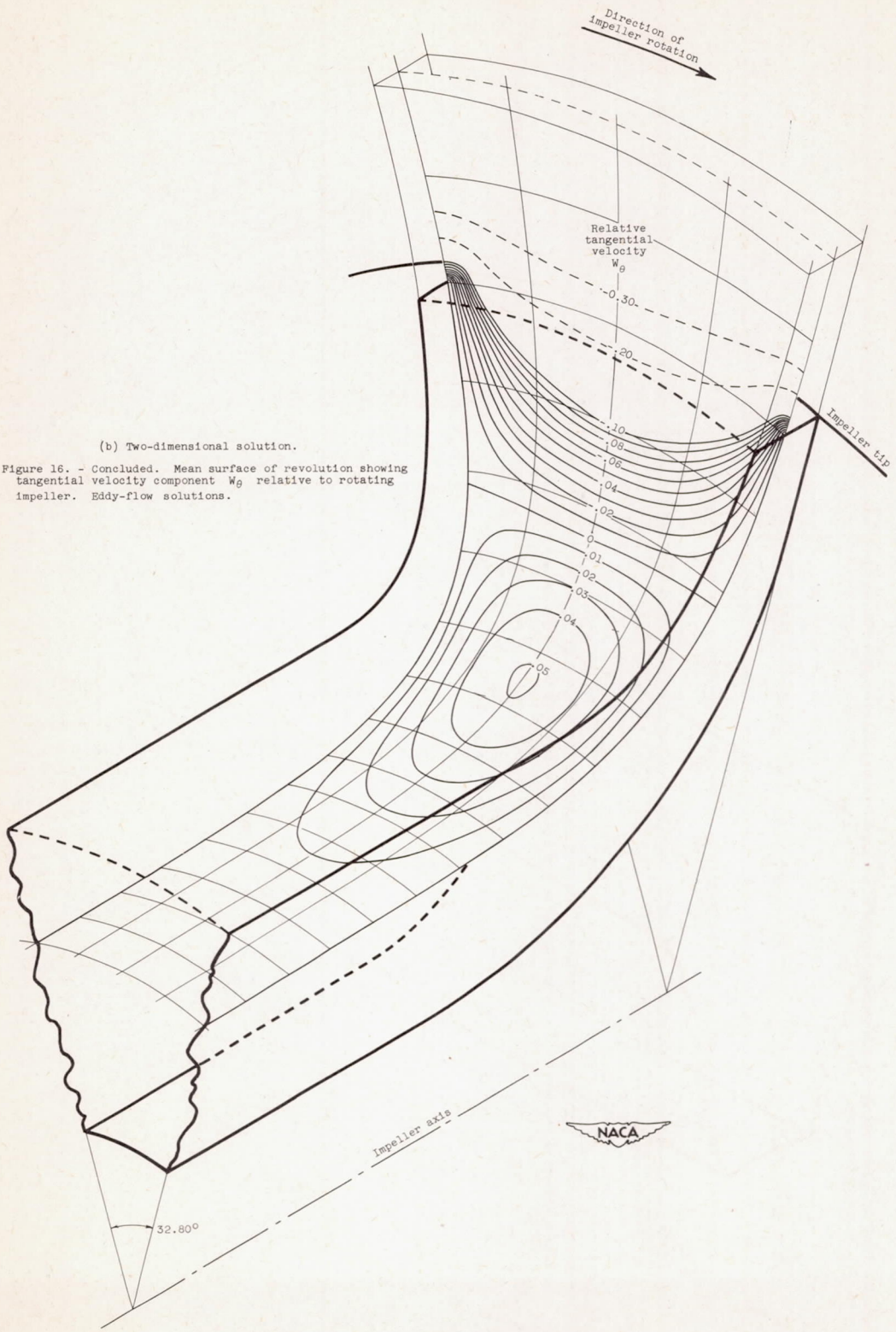

(b) Two-dimensional solution.

Figure 16. - Concluded. Mean surface of revolution showing tangential velocity component W_θ relative to rotating impeller. Eddy-flow solutions.

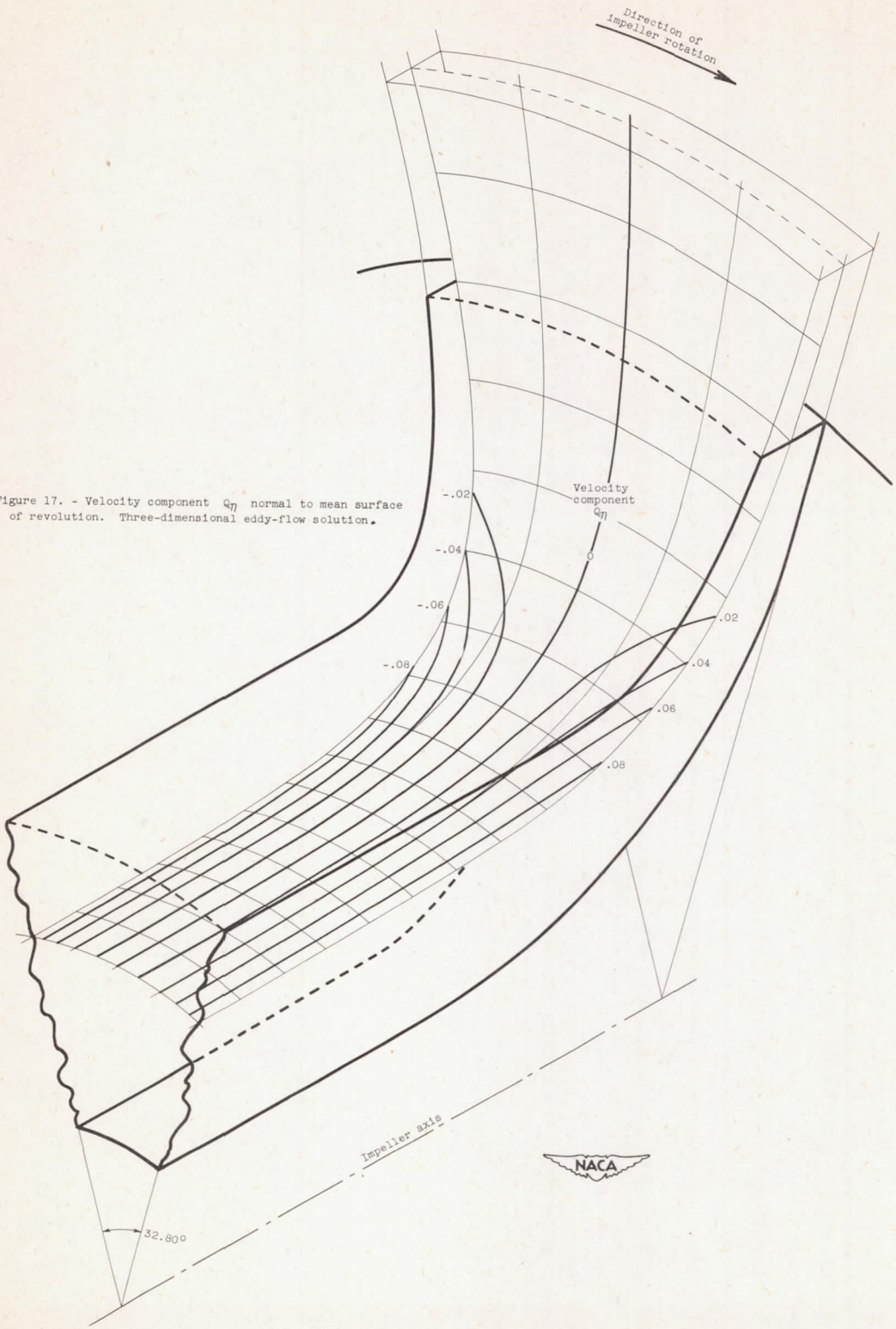

Figure 17. - Velocity component Q_η normal to mean surface of revolution. Three-dimensional eddy-flow solution.

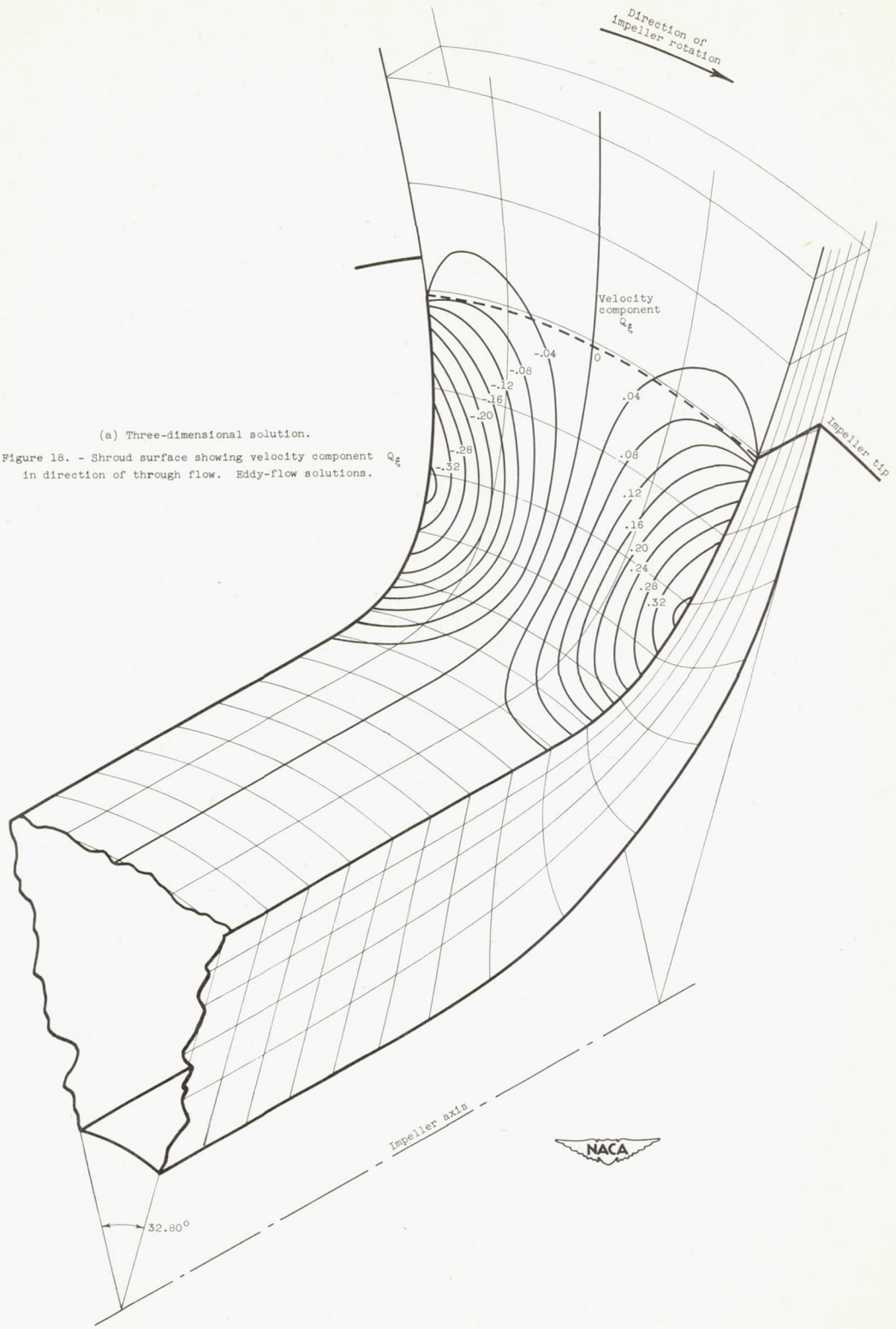

(a) Three-dimensional solution.

Figure 18. - Shroud surface showing velocity component Q_ξ in direction of through flow. Eddy-flow solutions.

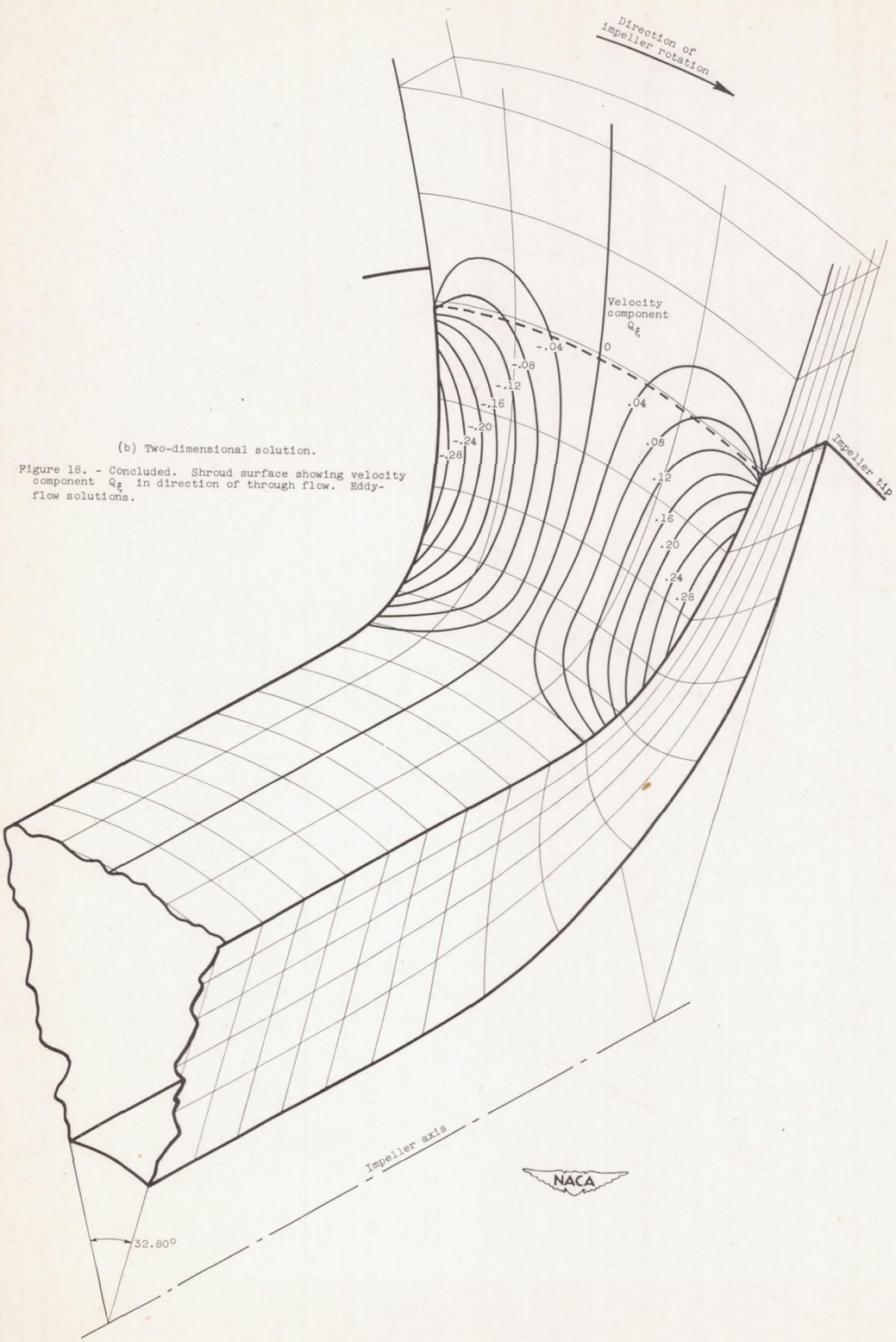

(b) Two-dimensional solution.

Figure 18. - Concluded. Shroud surface showing velocity component Q_ξ in direction of through flow. Eddy-flow solutions.

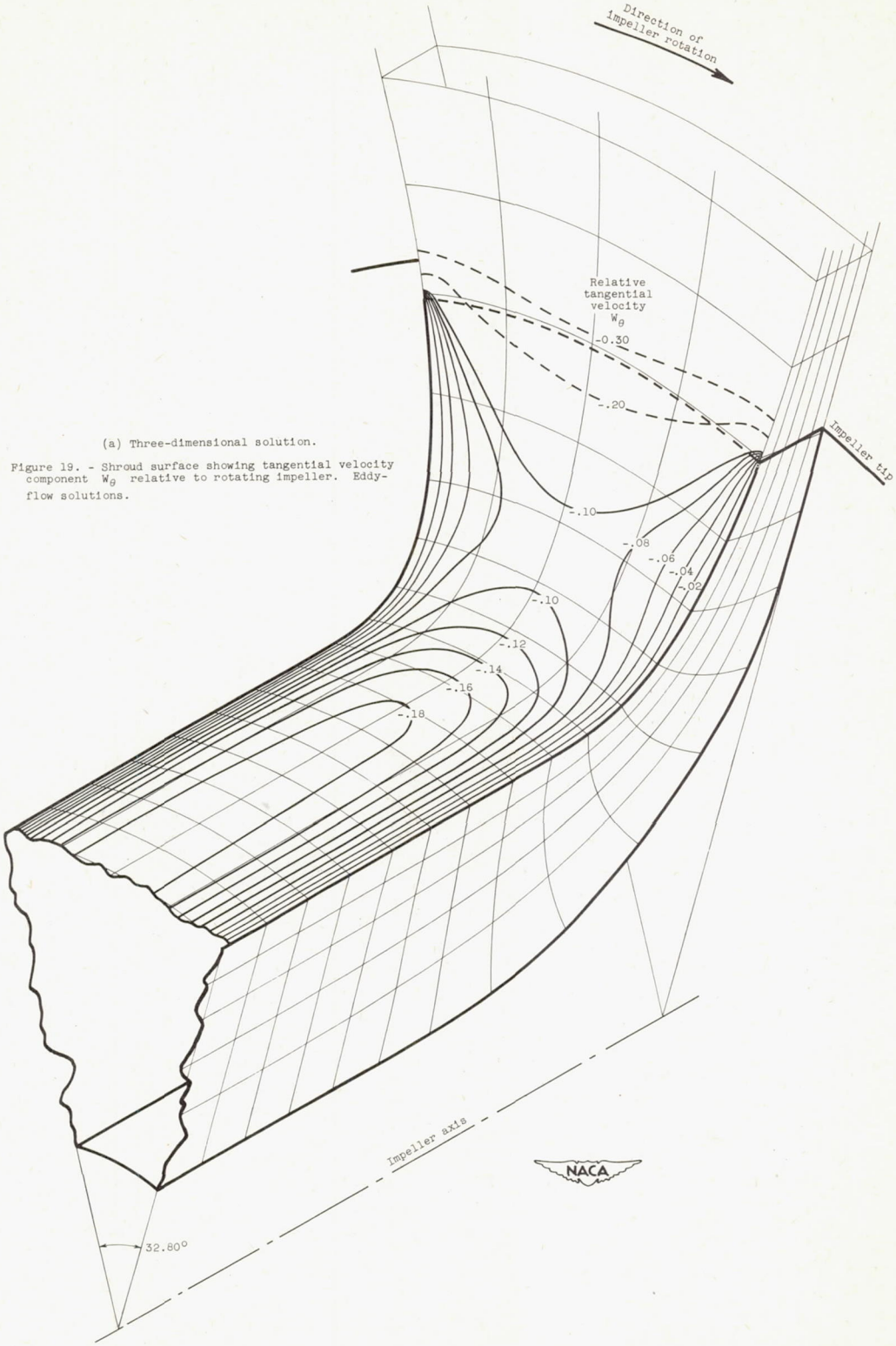

(a) Three-dimensional solution.

Figure 19. - Shroud surface showing tangential velocity component W_θ relative to rotating impeller. Eddy-flow solutions.

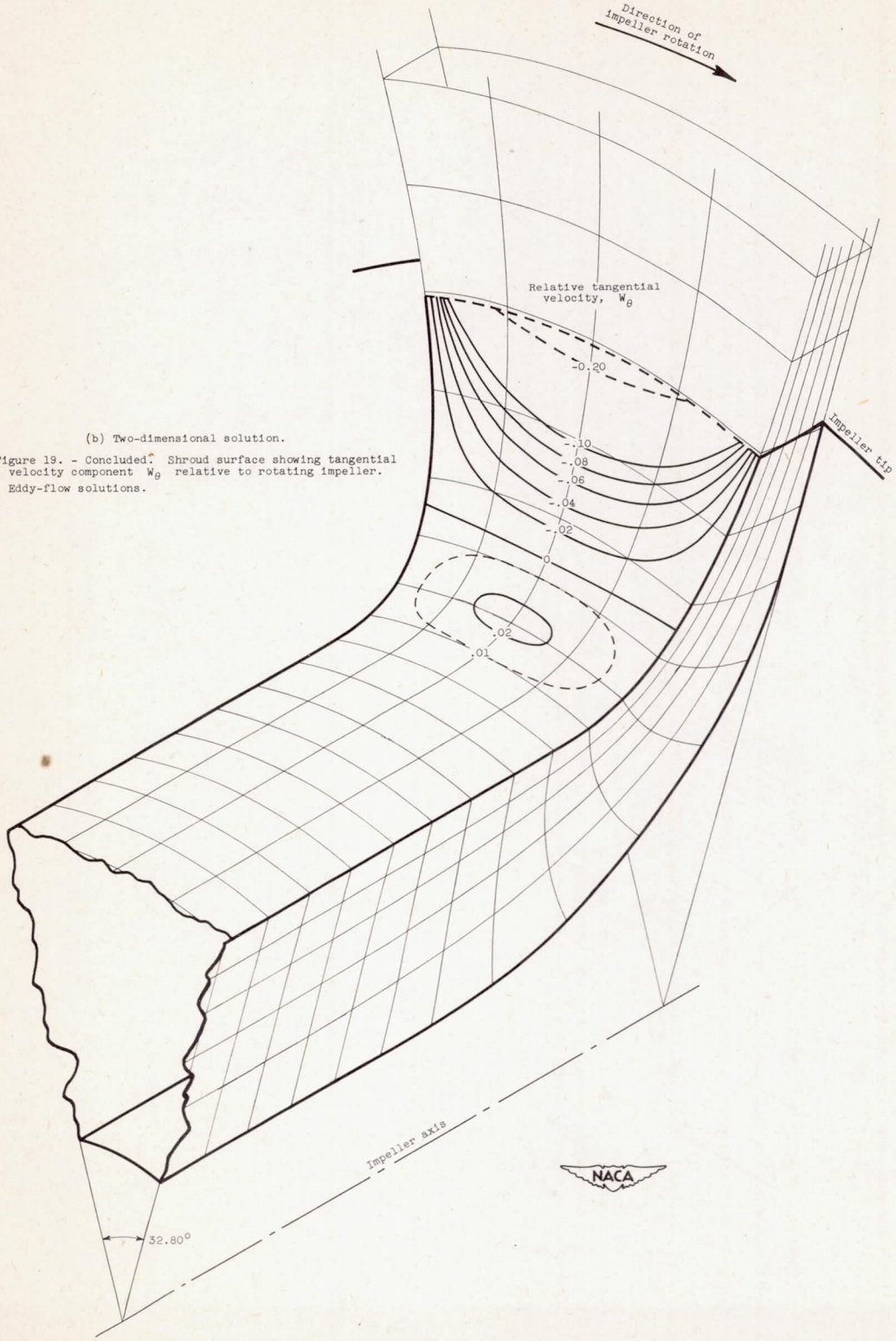

(b) Two-dimensional solution.

Figure 19. - Concluded. Shroud surface showing tangential velocity component W_θ relative to rotating impeller. Eddy-flow solutions.